Revised Manuscript: June 5th, 2020 edits to 2017-12-16129G with Corresponding author

Adaptable hemodynamic endothelial cells for organogenesis and tumorigenesis

Brisa Palikuqi[1], Duc-Huy T. Nguyen[1], Ge Li[1], Ryan Schreiner[1,2], Alessandro F. Pellegata[3], Ying Liu[1], David Redmond[1], Fuqiang Geng[1], Yang Lin[1], Jesus M. Gómez-Salinero[1], Masataka Yokoyama[1], Paul Zumbo[4], Tuo Zhang[5], Balvir Kunar[1], Mavee Witherspoon[6], Teng Han[6], Alfonso M. Tedeschi[3], Federico Scottoni[3], Steven Lipkin[6], Lukas Dow[6], Olivier Elemento[7], Jenny Z. Xiang[5], Koji Shido[1], Jason Spence[9], Qiao J. Zhou[1], Robert E. Schwartz[1,8], Paolo De Coppi[3,10], Sina Y. Rabbany[1,11], and Shahin Rafii[1*]

*** Corresponding Author:**
Shahin Rafii, 1300 York Avenue, Weill Cornell Medicine, NY, NY 10065
Email: srafii@med.cornell.edu

1) Division of Regenerative Medicine, Ansary Stem Cell Institute, Weill Cornell Medicine (WCM), New York, NY, 10065

2) Department of Ophthalmology, Margaret Dyson Vision Research Institute, Weill Cornell Medicine, New York, NY 10065

3) Stem Cell and Regenerative Medicine Section, Great Ormond Street Institute of Child Health, University College of London, London.

4) Applied Bioinformatics Core, Department of Physiology and Biophysics, Weill Medical Medicine, New York, NY, 10065

5) Genomics Resources Core Facility, Weill Cornell Medicine, New York, NY 10065

6) Sandra and Edward Meyer Cancer Center, Department of Medicine, Weill Cornell Graduate School of Medical Sciences, Department of Biochemistry, Weill Cornell Medicine, New York, NY

7) Caryl and Israel Englander Institute for Precision Medicine, Institute for Computational Biomedicine, Department of Physiology and Biophysics, Weill Cornell Medicine, New York, NY

8) Department of physiology, physics and system biology, Weill Cornell Medicine, New York NY 10065

9) Cell and Developmental Biology, University of Michigan School of Medicine, Ann Arbor, MI, 48109

10) Specialist neonatal and paediatric surgery, Great Ormond Street Hospital for Children NHS Foundation Trust, London, UK.

11) Bioengineering Program, DeMatteis School of Engineering and Applied Science, Hofstra University, NY 11549

Abstract:

Endothelial cells (ECs) adopt tissue-specific properties to instruct organ development[1,2]. This adaptability is lost in adult ECs and they fail to vascularize tissues in an organotypic manner. Here, we show that reactivation of embryonic-restricted ETS variant 2-transcription factor (ETV2)[3] in mature human ECs in three-dimensional (3D) Laminin-Entactin-CollagenIV (L.E.C) matrix "Resets" these stringent ECs into amenable vascular ECs (R-VECs), forming perfusable and adaptable vascular plexi. ETV2 via chromatin remodeling induces tubulogenic pathways, including Rap1-activation[4,5], promoting durable lumen formation. In 3D matrices, without the constraints of bioprinted scaffolds, R-VECs self-assemble into stable multi-layered vascular networks within large-volume sizable microfluidic chambers capable of transporting human blood. *In vivo,* implanted R-VEC self-organize into pericyte-coated vessels that functionally anastomose to host circulation and manifest long-lasting patterning, without malformations or angiomas. R-VECs, without the need for restrictive synthetic semipermeable membranes, directly interact with the cells within 3D cocultured organoids, establishing an Organ-On-VascularNet platform. R-VECs physiologically perfuse human pancreatic islets, vascularize decellularized intestines, and arborize normal and tumor organoids. Through scRNA-sequencing, we demonstrate that R-VECs establish an adaptive vascular niche, differentially adjusting and conforming to tissue-specific organoids and tumoroids. Deciphering the cross-talk between R-VECs and parenchymal cells facilitates the identification of EC heterogeneity determinants and warrants metabolic, immunological and physiochemical studies and screens, setting the stage for therapeutic organ repair and tumor targeting.

Main

Endothelial cells (ECs) in zonated capillaries sustain tissue-specific homeostasis and supply angiocrine factors to guide organ regeneration[1,2]. In contrast, maladaptation of ECs contributes to fibrosis and tumor progression[6,7]. The mechanism(s) by which ECs acquire adaptive tissue-specific heterogeneity or maladapt within the tumor microenvironment are unknown. Uncovering the molecular determinants of vascular heterogeneity, requires generation of malleable and perfusable vascular networks, that are responsive and can conform to microenvironmental and biophysical signals[8].

Attempts to uncover the cross-talk of adult ECs with non-vascular cells through generation of decellularized scaffolds[9,10], Organ-On-Chip models[11,12], 3D-bioprinting, as well as normal[13] and malignant organoids[14] cultures have confronted with hurdles. In these approaches, ECs are deprived of the cellular freedom to directly interact with parenchymal and tumor cells, due to physical constraints imposed by artificial semipermeable biomaterials, low-volume microfluidic devices and lack of adaptive ECs[11]. Moreover, the use of non-physiological matrices, such as Matrigel, poses roadblocks for translation to the clinic. Thus, transcriptional resetting of the adult human ECs to generate conformable and tubulogenic ECs in defined matrices will permit the unraveling of vascular diversity and therapeutic regeneration.

During development, the ETV2 transcription factor (TF) functions as a pioneer TF inducing vascular cell fate and lumen morphogenesis[3,15]. ETV2 is expressed in ECs during vasculogenesis and is turned off mid-gestation, when the primitive capillary networks are established[15] and is not expressed in the adult ECs. Transient re-introduction of ETV2 in parenchymal cells induces a stable EC fate[16]. Here, we show that in addition to specifying vascular fate, reactivation of ETV2 resets mature adult human vascular ECs (VECs) to embryonic-like malleable vasculogenic ECs, hereafter referred to as “Reset-VECs” (R-VECs). R-VECs self-organize into adaptable large volume 3D-vascular networks that can transport human blood and physiologically arborize decellularized tissues, islets, normal and malignant organoids and form durable capillaries *in vivo*.

R-VECs establish stable vessels *in vitro*

Human ECs transduced with lentiviral ETV2 form functional durable and adaptable 3D vessels by transitioning through 3 stages (**Fig. 1a, Extended Fig. 1a**). At the first induction stage, ETV2 upregulates vasculogenic and tubulogenic factors in flat EC cultures. During the 2nd remodeling stage, R-VECs placed in matrices, self-assemble into patterned and lumenized 3D vessels. At the 3rd stage, R-VECs are non-proliferative, maintaining stabilized and adaptive 3D capillaries (**Extended Fig. 1b**).

Human umbilical vein ECs (HUVECs) expressing ETV2, showed a 50-fold increase in vessel area formation over 8 weeks compared to naïve HUVECs, which did not form durable vessels in any of tested media **(Fig. 1b-c, Extended Fig. 1c-d, Video 1a).** Additionally, adult human mature EC populations isolated from adipose, cardiac, aortic, and dermal tissues transduced with ETV2, formed long-lasting and patterned

R-VEC plexi (**Extended Fig. 1e-g**). Next, we determined whether R-VEC vessel formation could be achieved without Matrigel. We identified a stoichiometrically defined ratio of Laminin, Entactin, and Collagen IV (L.E.C) matrices, which is sufficient for the self-assembly of R-VECs into lumenized vessels similar to those formed in Matrigel (**Fig. 1d, Extended Fig. 1h**). Confocal and electron microscopy showed that R-VECs organized into vessels with continuous patent lumen with proper polarity on both Matrigel and L.E.C matrix (**Fig. 1e, Extended Fig. 1i).** Moreover, ETV2 transduction reduces stiffness in adult ECs as measured by atomic force microscopy (AFM), facilitating lumen formation (**Extended Fig. 1j**). To assess the unique activity of ETV2 in promoting tubulogenesis, we transduced human ECs with another ETS-TF, *ETS1.* To test whether survival of ECs could drive lumen formation, HUVECs were also transduced with constitutively active myristoylated-AKT1 (*myr*AKT1). Neither *ETS1* nor *myr*AKT1 reset ECs to form stable vessels **(Extended Fig. 1k-m**).

We quantified the ETV2 mRNA and protein levels of R-VECs from stage 1 to 3 (**Extended Fig. 2a-d**). ETV2 protein levels peaked during stage 2 but were spontaneously downregulated by >90% at stage 3, which could not be accounted for by the minor drop in ETV2 mRNA levels (**Extended Fig. 2a-d**). Proteasome inhibitor MG132 restored ETV2 protein levels six-fold, indicating proteasomal proteolysis regulates ETV2 expression (**Extended Fig. 2e-f**). To examine if short-term ETV2 induction is sufficient to generate R-VECs, we used a reverse tet-transactivator (rtTA)-doxycycline (dox) inducible system, whereby dox induces ETV2 expression (iR-VECs) (**Extended Fig. 2g-h)**. ETV2 induction was only transiently required until the first week of stage 2; after that, iR-VECs sustain their stability without continuous ETV2 induction (**Extended Fig. 2i-k**).

Thus, short-term ETV2 expression confers adult ECs with the capacity to self-congregate into stable and patterned vessels without modulating survival, proliferation and without the physical constraints of artificial scaffolds and restrictive synthetic barriers.

R-VECs build durable vessels *in vivo*

SCID-beige mice were implanted subcutaneously with mCherry- or GFP-labeled control human ECs or R-VECs suspended in L.E.C matrix. One to five-months post-implantation, R-VECs, but not CTRL-ECs, self-organized into long-lasting patterned vessels *in vivo***.** Intravital injection of R-VEC implanted mice with an antibody directed to human VEcad (hVEcad) showed that R-VEC vessels anastomose to the Endomucin^{+} mouse vasculature, establishing functional mosaic perfused vessels throughout the plug (**Fig. 1f-h, Extended Fig. 3a**)**.** R-VEC vessels are invested by mouse perivascular cells, with larger arterioles covered with a thicker layer of smooth muscle cells and less coverage in smaller capillaries (**Extended Fig. 3b-c**). iR-VECs also assembled into stable vessels in L.E.C, and one week of dox *in vivo* was sufficient to retain vascular stability (**Extended Fig. 3d-e**). R-VEC and iR-VEC vessels in *in vivo* plugs were non-leaky and patent when mice were intravenously injected with 70 kDa dextran. By contrast, K-RAS transduced

human ECs formed leaky and disorganized vessels, reminiscent of hemangiomas (**Extended Fig. 3f**). Unlike K-RAS implanted plugs, R-VEC implants did not manifest aberrant growth, hemangiomas, or tumors, while also retaining perfused and organized vessels for 10 months (**Extended Fig. 4a-e**). Therefore, R-VECs form durable, anastomosed and structurally pericyte-covered normal capillaries without vascular anomalies or tumors.

R-VECs arborize decellularized scaffolds

We examined whether R-VECs could functionally arborize decellularized tissues. While large vessels in the decellularized scaffolds can be colonized with ECs, it is challenging to vascularize the profuse smaller capillaries[9]. Stage 1 R-VECs, but not CTRL-ECs, fully populated the narrow small capillaries evenly throughout the decellularized rat intestine scaffolds *ex vivo* (**Fig. 1i-j, Extended Fig. 5a-d**). After 1 week of *ex vivo* culture, the re-vascularized intestinal explants were implanted in the omentum of immunocompromised mice. Intravital anti-human VEcadherin (VEcad) staining at 1 and 4 weeks, showed that R-VEC vascularized scaffolds retained their patency and anastomosed to the mouse vasculature (**Extended Fig. 5e-f**). At 4 weeks, R-VEC vessels persisted at a higher rate *in vivo* due to their integrity and low apoptosis rate (**Extended Fig. 5g**). Thus, R-VECs enable physiological arborization of decellularized tissues for therapeutic regeneration.

ETV2 transcriptionally remodels ECs

To uncover the mechanism of ETV2 driven vascular resetting, we performed RNA-sequencing (RNA-seq) analysis of stage 1 R-VECs and CTRL-ECs (**Fig. 2a-c**). Gene ontology (GO) analyses revealed the upregulation of genes in pathways regulating vasculogenesis, angiogenesis, GTPase activity, extracellular matrix remodeling, and response to mechanical stimuli (**Fig. 2b-c, Extended Fig. 6a-b).** At stage 1, R-VECs maintain their vascular identity by switching on EC-specific genes (**Extended Fig. 6c**). Upon ETV2 induction, a group of 490 genes was differentially expressed among various tissue-specific adult human ECs, including cardiac, dermal, aortic, pulmonary and adipose-derived R-VECs (**Fig. 2d, Extended Fig. 6d).** ChIP-seq analysis of K4me3, K27ac and K27me3 histone modifications on both R-VECs and CTRL-ECs revealed binding of ETV2 to promoters of several differentially expressed vascular-specific genes, and to promoters of pro-tubulogenesis genes, which are silenced in mature ECs **(Fig. 2c,e, Extended Fig. 6e-h).** Therefore, ETV2 resets the chromatin and transcriptome of mature ECs with direct re-activation of suppressed tubulogenic and vasculogenic genes.

Upon ETV2 transduction, RASIP1 and three GEFs involved in small GTPase Rap1 activation, RASGRP2, RASGRP3 and RAPGEF5, crucial for lumen formation[4,5], were upregulated in all tissue-specific ECs (**Fig. 2c-d**). Similarly, differentially expressed genes in the Rap1 pathway, were found in ETV2 positive ECs isolated from ETV2-venus reporter mouse embryos at embryonic stage of 9.5 (E9.5) (**Extended Fig.**

7a-b). ChIP-seq analysis of stage 1 R-VECs confirmed direct binding of ETV2 to promoters of RASGRP3 and RASIP1 and subsequent increase in K4me3 and K27ac histone marks at these genes **(Fig. 2e).** A pull-down of active Rap1-GTP of stage 1 R-VECs, showed a higher level of active Rap1-GTP in R-VECs compared to naive ECs (**Fig. 2f**). Vessel formation was reduced, and no lumen was present following treatment with the Rap1-inhibitor GGTI298 (**Fig. 2g-h**). Likewise, knockdown of RASGRP3 by shRNA disrupted R-VEC mediated tubulogenesis (**Extended Fig. 7c**). Therefore, ETV2 potentiates lumen formation, in part, through upregulation of Rap1-GEFs.

In vitro, stage 3 R-VECs upregulate genes involved in mechanosensing (*PIEZO2*, *KLF2*, and *KLF4*) and EC-remodeling (*ATF3*), which are absent in cultured mature ECs (**Extended Fig. 7d**). This was further confirmed by isolating R-VECs from *in vivo* plugs and comparing their transcriptome to freshly isolated HUVECs and R-VEC stage 3 stable vessels (**Extended Fig. 7d**). Notably, the genes upregulated in stage 3 R-VECs (*PIEZO2*, *KLF2* and *KLF4*) were bound by ETV2 and epigenetically primed for expression in stage 1 2D R-VECs (**Extended Fig. 7e**). Thus, ETV2 recapitulates the chromatin purview of mature ECs into an *in vivo* physiological configuration that is reminiscent of generic vasculogenic ECs responsive and conforming to microenvironmental cues.

R-VEC vessels are hemodynamic

We tested the competence of R-VEC vessels to self-assemble into vascular networks in the absence of pre-patterned scaffolds and synthetic barriers to sustain a laminar flow *in vitro* in large volume microfluidic devices. R-VECs or CTRL-ECs were seeded in a 5x3x1 millimeter microfluidic device accommodating >45,000 stage 1 ECs within a sizable volume of 15 microliters of fibrin gel[17] (**Fig. 3a**). Within 3 days, R-VECs self-organized into a multi-layered and interconnected vascular plexus preserving their 3D-lumenized stability (**Fig. 3b-d**). Notably, R-VEC vessels allowed the gravity-driven transport of heparinized whole human peripheral blood, with a full complement of plasma, platelets, WBCs and RBCs (**Fig. 3e and Video 1b-c**). During the transportation of blood, R-VEC capillary networks sustained their vascular integrity and were hemodynamically stable throughout the inlet to the outlet chambers of the microfluidic device; enduring the force of blood flow without collapse, regression or thrombosis. Thus, R-VECs bolster hemodynamic vascularization of tissues, setting the stage for a model of the Organ-On-VascularNet platform.

R-VECs physiologically vascularize islets

We assessed the potential of R-VECs to functionally vascularize human islets in the perfusable microfluidic devices. Current Organ-On-Chip devices[11,12] segregates ECs from parenchymal cells with physical barriers, and thus are unsuitable for studying islets, which require active interaction with ECs to maintain function[18]. We accommodated ~40 human islets alone or in presence of CTRL-EC or R-VECs in

substantially large 15 μl microfluidic devices (**Fig. 3f**). Within 3 days, R-VEC but not CRTL-EC, arborized islets with continuous 3D vascular networks, delving deep into islets, metabolically irrigating insulin-producing β-cells (**Fig. 3g-j, Video 2b-f**). Heparinized human blood traveled through the R-VEC co-opted islets, with intact haematopoietic cells crisscrossing the vascularized islets (**Fig. 3h, Video 2b-e**).

Employing a glucose stimulation test to assess islet function (**Fig. 3k**), we show that islets arborized with R-VECs responded to high glucose by secreting insulin, as measured at the device outlet at 9 and 24 minutes of stimulation **(Fig. 3k).** There was a 7-fold increase of insulin secretion in glucose-stimulated R-VEC co-opted islets, but not CTRL-ECs or islet-alone cultures (**Fig. 3l**). Co-cultured islet explants arborized by R-VECs in static Matrigel droplets yielded similar results **(Extended Fig. 8a-e).** Thus, R-VECs self-congregate in sizable large volume microfluidic devices into hemodynamically stable vessels, physiologically perfusing and sustaining glucose-sensing human β–cells.

R-VECs arborize organoids and tumoroids

We interrogated R-VECs capacity to functionally vascularize human normal or malignant organoids to model tissue- and tumor- specific adaptive responses of ECs; setting the stage for organ regeneration. Normal human colon organoids (hCOs) were established and maintained from healthy human colon crypts[19,20] (**Extended Fig. 8f)**. Next, hCOs were mixed with either CTRL-ECs or stage 1 R-VECs in static 50 μl of Matrigel or L.E.C. matrix droplets (**Fig. 4a)**. R-VECs, but not CTRL-ECs, sustained the arborization of hCOs throughout the matrix droplet with a higher vessel area (**Fig. 4b-c, Video 3a).** R-VECs were found to interact with the hCOs at a much higher rate, as tracked over a 72-hour time-lapse video (**Fig. 4d, Video 3b).** Colon organoid area was higher in the presence of R-VECs, with no change in differentiation of colon organoids stem and progenitor markers (**Fig. 4e, Extended Fig. 8g**). R-VECs also arborized mouse small intestinal organoids with a coverage of higher vessel area and the number of R-VEC sprouts per organoid (**Extended Fig. 8h-j).** Thus, R-VECs, instructively sustain proliferation and integrity of hCOs, while preserving their differentiation status.

Tumor vasculature is composed of abnormal capillaries that supply aberrant factors that instigate tumor growth[7]. To determine whether R-VECs can acquire and report on the maladapted features of tumor vessels, we co-mingled stage 1 R-VECs with patient-derived colorectal cancer organoids (hCRCOs) (**Fig. 4f, Video 3c).** Within 24 hours, R-VECs, but not CTRL-ECs migrated and infiltrated tumor organoids **(Video 3c)**. Similar to hCOs, vessel area and interaction of R-VECs with hCRCOs was higher than that of CTRL-EC (**Fig. 4g, Extended Fig. 8l, Video 3c).** Staining for the epithelial marker EpCAM, revealed the intimate cell-cell interactions between the tumoroids and R-VECs, with a higher percentage of EdU^+ proliferating tumor cells in the R-VEC co-cultures (**Fig. 4h, Extended Fig. 8k**). Hence, R-VECs establish an adaptive 3D vascular niche to decipher the cross-talk between ECs and normal or tumor organoids.

R-VECs adapt to organoids and tumoroids

We performed single-cell RNA sequencing (scRNA-seq) on the 3D R-VEC-vascularized normal or tumor colon organoids to assess R-VEC adaptability. R-VECs cultured alone and those co-cultured with hCOs or hCRCOs for 7 days, were isolated and subjected to scRNA-seq using 10X Chromium platform (**Extended Fig. 9a, Extended Fig. 10a**). The ECs were identified as cells expressing VEcad, CD31, and VEGFR2 and epithelial cells by EpCAM, CDH1 and KRT19 (**Extended Fig. 9b-e, Extended Fig. 10b-e).** Identity of hCOs was validated by SATB2, CA4, CA2 among others (**Extended Fig. 9f**).

R-VECs co-cultured with malignant or normal organoids, manifested changes in their clustering patterns and gene expression when compared to R-VECs alone (**Fig. 4i-n**). R-VECs which interacted with hCOs, were enriched with EC-organotypic markers, including *PLVAP* and *TFF3* (cluster 5)[1,21] (**Fig. 4i-k**)**.** By contrast, R-VECs arborizing hCRCOs were enriched in clusters with prototypical tumor EC attributes, including *ID1*, *JUNB* and *ADAMTS4* (cluster 8), while genes responsible for junctional integrity, such as *Claudin-5* (cluster 5, cluster 7) were selected against[22] (**Fig. 4l-n)**. Reciprocally, in response to association with R-VECs, colon tumor cells upregulated markers linked to poorer prognosis and higher metastasis, including higher levels of *MSLN*[23], and lower levels of *MT1G*, *MT1X* and *MT2A*[24] (**Extended Fig. 10f-h).** Thus, R-VECs create an adaptable 3D vascular niche that conforms to microenvironmental stimuli **(Fig. 4o)**.

We have devised hemodynamic self-organizing large volume 3D vascular networks in defined Matrigel-free L.E.C. matrix, without the constraints of synthetic scaffolds and membranes, authorizing direct cellular interaction of ECs with parenchymal and tumor cells. Re-introduction of ETV2 -silenced during fetal development- into adult human ECs induces a 'molecular reset' of tubulogenic and adaptability attributes, which are extinguished in cultured mature ECs[4,5]. R-VECs activate the Rap1 pathway through Rap1-GEFs and RASIP1 effector, to choreograph durable lumen formation in a flow- and pericyte- independent manner. ETV2 resets the vasculogenic memory to a primitive stage rendering R-VECs receptive to microenvironmental cues[1,2]. In stabilized R-VEC vessels, ETV2 expression was diminished through proteasomal proteolysis, suggesting that transient ETV2 expression suffices to reset ECs into a plastic and adaptive state.

R-VECs capacity to self-assemble into perfusable vascular networks that can transport human peripheral blood, enables 3D physiological vascularization of scalable and organ-level micro- and macro-fluidic manifolds. This licenses R-VECs to recapitulate the physiochemical and multicellular geometry of blood perfusable vascular niches that by deploying angiocrine factors, instructively enhance the frequency of co-cultured organoids. In turn, R-VECs conform to signals emanating from organoids or tumoroids. Reciprocally, tumor cells upregulate markers associated with poor outcomes in response to signals induced by subverted R-VECs. Hence, the R-VEC Organ-On-VascularNet platform overcomes the restrictive

constraints of costly Organ-On-Chip models whose design interfere with direct cellular interaction of ECs with non-vascular cells.

Blood perfusable pericyte coated R-VEC:organoid coculture serve as a biologically tissue-specific platform for delivery of engineered immune cells, such as CAR-T cells, chemotherapeutic agents, and uncovering pathogenesis of COVID19 microangiopathy. The durable tubulogenic, scalability, hemodynamic blood perfusibility, geometrical malleability, media compatibility and adaptability of R-VECs, capable of vascularizing normal and malignant organoids or decellularized scaffolds, will lay the foundation for physiological, metabolic and immunological studies and pharmaceutical screening. The R-VEC Organ-On-VascularNet model permits *ex vivo* construction of functional and perfused implantable tissues, opening a new chapter in modern "Translational Vascular Medicine", for tissue-specific regeneration and targeting corrupted tumor vascular niches.

Figure Legends:

Figure 1. R-VECs self-assemble into 3D durable vessels *in vitro* and *in vivo*.

a) Experimental set up for vessel formation. 10^5 CTRL-EC or R-VECs were plated on Matrigel in StemSpan tube formation media (**Supplementary Data 3**). **b)** Z-stack of R-VEC vessels at week 16. **c)** Quantification of tube formation CTRL-EC (HUVECs) and R-VEC (HUVEC-ETV2). **d)** Quantification of R-VEC vessels on Matrigel and defined laminin, entactin, collagenIV (L.E.C.) matrix. **e)** Electron microscopy of stage 3 vessels on Matrigel and L.E.C. L=Lumen**. f)** Schematic of *in vivo* plug experiment where fluorescently-labeled CTRL-ECs or R-VECs (hEC, GFP) were subcutaneously injected as a single cell L.E.C. suspension into SCID beige mice. Whole mount confocal images of R-VEC plugs and CTRL-EC plugs at 5 months. Fluorescently labeled antibody against human VEcad (hVEcad) was injected retro-orbitally before sacrifice. **g)** Orthogonal projection depicting anastomosis of mouse and hVEcad vessels. Sections were post-stained for mEndomucin. **h)** Quantification of human vessel area in the plugs. **i)** Experimental procedure of decellularized intestines cultures'. R-VECs repopulated the vasculature lining blood vessels, including in distal capillaries. At day 7 the bioreactors were stained for human CD31 (hCD31), imaged and **j)** quantified. Data are represented as mean +/- S.E.M. ns=not significant; *<0.05, **<0.01, and ***<0.001. For statistics see **Supplementary Data 2.**

Figure 2. Transcriptome and epigenetic analyses of R-VEC signatures

a) Schema of RNA and ChIP-sequencing performed on R-VECs and CTRL-ECs. **b)** RNA-seq of R-VECs or CRTL-HUVECs in stage 1 (2D monolayers). GO Term analysis was performed on differentially expressed (DE) genes. GO categories are ordered based on number of DE genes. **c)** Heatmap of genes in one top GO

category. Values are log2 normalized counts per million, centered and scaled by row. ETV2 binding from ChIP-seq at the promoter of each differentially expressed gene is shown in the yellow-green heatmap. **d)** Heatmap of 490 DE genes across different tissue ECs (stage 1 induction) upon ETV2 expression. Tissue-adjusted log2 CPMs, centered and scaled by row. **e)** ETV2 ChIP-seq on R-VECs during stage 1 induction phase (2D) using an anti-flag antibody or mouse IgG as control. ChIP for H3K4me3, H3K27ac and H3K27me3 was performed on both CTRL-EC and on R-VEC at the induction stage 1 (2D). Enriched regions were analyzed by ChIP-sequencing. Bars underneath peaks represent significantly changed regions. Promoter regions bound by ETV2 are highlighted in cream. Track range ETV2/K27me3/K27ac, 0-0.3; K4me3/input/IgG, 0-1. **f)** Western blot for active Rap1-GTP compared to total Rap1 input for stage 1 2D HUVEC-CTRL and HUVEC-ETV2. **g)** Quantification of R-VEC vessel formation with Rap1 inhibitor or DMSO. **h)** Z-stack confocal images and electron microscopy images of R-VEC vessels with Rap1 inhibitor or DMSO at 4W. Red circles point at orthogonal cross-sections. Data are represented as mean +/- S.E.M. ns=not significant; *<0.05, **<0.01, and ***<0.001. For statistics see **Supplementary Data 2.**

Figure 3. R-VECs hemodynamically and physiologically vascularize human islets

a) Overview of microfluidic device - measuring 5mmx3mmx1mm and holding 15 µl fibrin gel. **b)** Representative images of devices with CTRL-ECs or R-VECs stained with hVEcad antibody at day 7. **c)** Orthogonal representation of intact lumen formation of R-VECs **d)** Quantification of vessel area in devices with CTRL-ECs vs R-VECs. **e)** 100µl of intact heparinized human peripheral blood composed of full complement of RBCs, WBCs, platelets and unperturbed plasma was injected and perfused through the R-VEC vessels. Representative image captured from live flow of blood through R-VECs (also **Video 1b-c**). **f)** Experimental set-up of co-seeding human islets with CTRL-ECs or R-VECs in microfluidic devices. **g)** Fluorescently labeled heparinized whole human blood (Red, Pkh26 Red Fluorescent dye) was perfused through the microfluidic devices (day 4) (also **Video 2c-d**)**. h)** Z-stack projections of whole devices of islet explants post-stained with EpCAM and VEcad (day 4). **i)** Zoomed in area of direct interaction of R-VECs with co-cultured islets in a microfluidic device. **j)** Single section and orthogonal projection of human islets vascularized by R-VECs in microfluidic device. **k)** Glucose stimulation test set-up in microfluidic devices. **l)** Insulin levels were measured at 2mM glucose as basal level and after 16.7mM glucose stimulation. * vs. Islets alone, $^{\#}$ vs. Islets + CTRL-EC **m)** Insulin fold change at the outlet, (insulin levels at 16.7 mM/insulin levels at 2mM), 9 min post high glucose stimulation. Data are represented as mean +/- S.E.M. ns=not significant; *<0.05, **<0.01, and ***, $^{\#\#\#}$<0.001. For statistics see **Supplementary Data 2.**

Figure 4. R-VECs arborize and conform to normal and tumor organoids.

a) CTRL-ECs or R-VECs were seeded with hCOs or hCRCOs in Matrigel droplets. **b)** Confocal Z-projections and **c)** zoomed images of hCOs alone, or co-cultured with CTRL-EC or R-VEC on day 8. **d)** Kinetics of area of CTRL-ECs or R-VECs interacting with hCOs in L.E.C. quantified over a 72-hour time-lapse. **e)** Quantification of colon area (as stained by EpCAM)/field on day 8. **f)** hCRCOs were seeded with CTRL-EC or R-VECs in Matrigel droplets. Confocal images of hCRCOs alone, or co-cultured with CTRL-EC or R-VECs post-stained for KRT20 at day 8 after a 4.5 hour EdU pulse. **g)** Kinetics of surface area of CTRL-ECs or R-VECs interacting with hCRCOs in Matrigel were quantified over a 78-hour time-lapse. **h)** Quantification of levels of EdU in hCRCOs alone, or co-cultured with CTRL-EC or R-VEC on day 8. **i)** Single-cell suspension R-VECs were cultured either alone or co-mingled with hCOs and submitted for scRNA sequencing on day 7. UMAP plots for EC fractions of R-VECs alone and R-VECs co-cultured with hCOs. **j)** ECs combined from R-VECs alone and R-VECs co-cultured with hCOs group in 9 unique clusters. **k)** Heatmap of DE genes from cluster 5, enriched among R-VECs in culture with hCOs. **l)** Single-cell suspension R-VECs were cultured either alone or co-mingled with hCRCOs and submitted for scRNA sequencing on day 7. UMAP plots for EC fraction of R-VECs alone and R-VECs co-cultured with hCRCOs. **m)** ECs combined from R-VECs alone and R-VECs co-cultured with normal colon organoids group in 8 unique clusters. **n)** Heatmap of DE genes from cluster 8, enriched among R-VECs in culture with hCRCOs. **o)** Schematic of R-VEC adaptive and maladaptive education. Data are represented as mean +/- S.E.M. ns=not significant; *<0.05, **<0.01, and ***<0.001. For statistics see **Supplementary Data 2.**

Extended Figure Legends:

Extended Figure 1. ETV2 uniquely confers mature human ECs with the ability to autonomously self-assemble into lumenized, durable and patterned vessels *in vitro* without the constraints of scaffolds

a) Overview of experimental set up for vessel formation *in vitro* for screen of different media, extracellular cellular matrix components and different tissue-specific ECs. **b)** The proliferation of GFP-transduced R-VEC and CTRL-EC at each stage of vessel formation. EdU^+ cells were quantified after a 16-hr EdU pulse. **c)** Time course of vessel formation on Matrigel for GFP^+ CTRL-EC and R-VECs over 8 weeks. **d)** Vessel formation using R-VEC or CTRL-EC in three different media (**Supplementary Data 3**): StemSpan with Knockout serum replacement and Cytokines, EGM-2 and complete EC media on Matrigel. R-VEC formed the most robust lumenized vessels in StemSpan with knockout serum replacement medium and cytokines, as compared to other media with serum. CTRL-EC failed to form stable vessels. **e)** Time course and **f)** quantification of tube formation for GFP^+ Adipose CTRL-EC and Adipose R-VEC on Matrigel. **g)** Representative images of tissue-specific GFP^+ R-VEC and CTRL-EC isolated from adult human heart (cardiac EC), aorta (aortic EC), and skin (dermal EC) demonstrated robust and stable vessels at 4 weeks on Matrigel. **h)** Representative images of GFP^+ R-VEC vessels formed on Matrigel or a pre-defined matrix of Laminin/Entactin and CollagenIV (L.E.C). **i)** Immunostaining of R-VEC-tubes displayed proper polarity with podocalyxin, apical (in red) and laminin, basal (in green). The right image is an orthogonal projection. **j)** Stiffness measurements by atomic force microscopy (AFM) of adult Adipose and HUVEC ECs with and without ETV2. In both cases, ETV2 cells are significantly less stiff than their counterparts. The abbreviated box plots indicate the interquartile range and median for each condition. **k)** HUVECs were transduced with either an empty vector, ETV2, *myr*AKT or ETS1 and used in a vessel formation assay. Western Blot analysis for expression of ETV2, p-AKT, total AKT and ETS1 in those cells. **l)** Representative images for ETS1 or *myr*AKT1 transduced GFP^+ HUVECs in a vessel formation assay on Matrigel. **m)** Quantification of vessel area for ETS-1, *myr*AKT and ETV2 (R-VEC) cells indicated that ETS-1-EC and *myr*AKT-EC fail to form robust vessel formation as compared to R-VEC. Data are represented as mean +/- S.E.M. ns = not significant; *<0.05, **<0.01, and ***<0.001. For statistics see **Supplementary Data 2.** For media formulations refer to **Supplementary Data 3.**

Extended Figure 2. Transient ETV2 expression in mature ECs is sufficient for the generation and maintenance of durable long-lasting R-VEC vessels *in vitro*

a) Schematic for ETV2 mRNA and protein levels assessment at each of the three stages of R-VEC vessel formation**. b)** Quantification of ETV2 mRNA levels at each stage of vessel formation. **c)** Western

Blot analysis and **d)** densitometric quantification of ETV2 protein levels at each stage of vessel formation. GAPDH was used as a loading control. **e)** A proteasome inhibitor (MG132) restored ETV2 levels by ~6 fold when added to R-VECs during the stabilization stage. **f)** Densitometric quantification of Western Blots in **e**. **g)** qRT-PCR and **h)** Western Blot assessment of ETV2 levels upon doxycycline removal. **i)** Representative images of GFP^+ iR-VECs on Matrigel with inducible ETV2 expression at 2 months. ETV2 was turned off at day 0, day 7 and at 4-weeks post start of the remodeling stage 2. **j)** Quantification of iR-VEC vessels at 2 months. **k)** Electron microscopy (EM) pictures of a lumen present both in vessels where doxycycline was continuously on and in vessels where doxycycline was removed after 1 month. Data are represented as mean +/- S.E.M. ns= not significant; *<0.05, **<0.01, and ***<0.001. For statistics see **Supplementary Data 2.** For media formulations refer to **Supplementary Data 3.**

Extended Figure 3. R-VEC vessels are functionally anastomosed and not leaky *in vivo.*

a) Fluorescently labeled R-VEC or CTRL-EC cells in L.E.C. were subcutaneously injected in the flank of SCID beige mice and retrieved at 2 months. Human-specific VEcad antibody (hVEcad) was injected intravitally right before sacrifice. Sections of the plugs were stained for mouse ECs with an anti-mouse endomucin antibody (mEndomucin), identifying properly organized human R-VECs anastomosing with mouse vessels (thickness=50 μm). Sections were also stained with the nuclear stain DAPI. **b)** Plugs in **a** were post-stained with hVEcad and a mouse Pdgfrβ antibody or **c)** mouse SMA antibody (thickness=50 μm). **d)** *In vivo* plug assay, where mice were subcutaneously injected with either control ECs (HUVECs transduced only with rtTA lentivirus) or stage 1 doxycycline-inducible-ETV2 ECs (iR-VECs: HUVECs transduced with both rtTA and inducible ETV2 lentivirus) in L.E.C. One group of mice was on doxycycline (ETV2 continuously on) and another group of mice was on doxycycline food diet for 1 week (ETV2 on) and then switched to regular food (ETV2 off). All mice were sacrificed 2-months post-implantation. Red indicates the GFP labeled human ECs, white: Anti-VEcad antibody that was retro-orbitally injected before sacrificing the mice**. e)** Quantification of vessel area for rtTA only plugs, mice on dox for 1 week, and mice continuously on doxycycline diet (ETV2 on). All mice were sacrificed 2-months post-implantation. **f)** 70 kDa fluorescent dextran in (blue) and human VEcad (in white) were injected in mice implanted with fluorescently labeled R-VECs (in red, 5-months post-implantation), iRVECs (in red, 1 week on dox food and sacrificed at 2 months) or K-RAS-HUVECs (K-RAS-EC) (in red, 2-weeks post-implantation) to assess anastomosis and leakiness of vessels. K-RAS-EC vessels showed dextran leakiness, while R-VEC and iR-VEC vessels exhibited patency and non-leakiness. Green arrows point at perfused mouse vessels that were also perfused with dextran. Data are represented as mean +/- S.E.M. ns= not significant; *<0.05, **<0.01, and ***<0.001. For statistics see **Supplementary Data 2.**

Extended Figure 4. Implanted R-VECs form stable vessels *in vivo* without features of vascular malformations, cysts, adenomas, hemangiomas or metastasis.

a) Representative images of non-hemorrhagic R-VEC plugs at 10 months and **b)** Whole-mount microscopy of R-VEC plugs at 10-months post perfusion with anti-human VEcad antibody (hVEcad). **c)** Representative H&E and Masson staining of R-VEC plugs at 10 months. There were no features of cysts or hemangiomas present in contrast to **d)** K-RAS-EC plugs (at 4 weeks) that formed an EC tumor. **e)** There was no metastasis to R-VECs other tissues 10-months post plug implantation and the tissues were assessed to be normal by H&E, Masson and Picrosirius staining.

Extended Figure 5. Decellularized intestinal scaffold re-endothelialized with R-VECs engraft *in vivo* upon omental implantation

a) Experimental procedure schematic of heterotopic implantation of decellularized intestinal scaffold vascularized using R-VECs. **b)** Harvested rat intestines were cannulated through lumen, mesenteric artery and mesenteric vein (scale bar 1cm). **c)** Decellularized intestine preserves native vasculature (green= GFP^+ R-VECs). **d)** Seeded GFP labeled R-VECs spread evenly and reach distal capillaries. **e)** Heterotopic implantation of re-endothelialized intestines in immunodeficient mice omentum shows engraftment after 1 and 4 weeks of GFP^+ R-VECs and anastomosis to the host vasculature as indicated by intravital intravenous injection of anti-human VEcad antibody (hVEcad). Representative H&E stainings show anatomical normal perfused vessels. **f)** Quantification of the area covered by R-VEC compared to CTRL-EC in implanted re-endothelialized intestines at 1 week and 4 weeks. **g)** Quantification of R-VEC and CTRL-EC proliferation and apoptosis in implanted re-endothelialized intestines at 1 and 4 weeks. Data are represented as mean ± S.E.M. ns=not significant; *<0.05, **<0.01, and ***<0.001. For statistics see **Supplementary Data 2.**

Extend Figure 6. ETV2 by directly binding to promoters and enhancers of target genes regulates differentially expressed genes in R-VECs.

a) Schema of RNA-sequencing performed on R-VECs and CTRL-ECs derived from different tissue-specific ECs during stage 1 induction phase (2D monolayers). **b)** R-VECs or CRTL-ECs were analyzed by RNA sequencing. Heatmaps of selected genes within top enriched GO categories. Values are log2 normalized counts per million, centered and scaled by row. ETV2 binding from ChIP-seq at the promoter of each differentially expressed gene is shown in the yellow-green heatmap. **c)** R-VECs retain essential EC fate genes at stage 1 induction phase across all tissue-specific ECs. The data is presented as $\log_2$ counts per million with no scaling by row or column. **d)** PCA plot based on the top 1000 most variable genes across ECs with and without ETV2 from different tissues during stage 1 induction, using $\log_2$ normalized counts per million (CPM) after subtracting tissue-specific effects using limma's removeBatchEffect function. **e)** ETV2

ChIP was performed on R-VECs using an anti-flag antibody at the induction stage 1 (2D), along with histone modification ChIP for H3K4me3 and H3K27ac. Enriched regions were analyzed by ChIP-sequencing. **f)** Genomic distribution of ETV2 peaks in R-VEC (Stage 1). The number in brackets is the number of ETV2 peaks in each region. **g)** Promoters bound by ETV2 have an increase in both K4me3 and K27ac. **h)** GO enrichment in genes with ETV2 binding at promoters are shown. For statistics, see **Supplementary Data 2.**

Extended Figure 7. ETV2 in R-VECs endow ECs with transcriptional adaptability and plasticity.
a) Diagram of EC sample preparation from ETV2 Venus reporter mice by FACS sorting. $ETV2^{pos}$ and $ETV2^{neg}$ ECs were sorted at day E9.5. ECs were sorted as non-haematopoietic $CD31^{+}CD45^{neg}$ cells. **b)** Heatmap of overlap of differentially expressed genes in $ETV2^{pos}$ vs. $ETV2^{neg}$ ECs at E9.5 and R-VECs (stage 1) vs. CTRL-EC from different tissues, using tissue-adjusted $\log_2$ CPMs, centered and scaled by row. **c)** Knockdown of RASGRP3 by two different shRNAs in R-VECs, shRNA against Luciferase was used as control. Vessel quantification upon RASGRP3 knockdown. **d)** Heatmap displaying overlapping differentially expressed genes from R-VEC at stabilization stage 3 (4 weeks) vs. R-VEC at induction stage 1, R-VECs *in vitro* pre-plug (stage 1 induction stage) vs. R-VECs in vivo in plugs (1 month), and freshly isolated vs. cultured HUVECs. Values represent tissue-adjusted $\log_2$ CPMs, centered and scaled by row. **e**) ChIP-sequencing depicting genes that are differentially expressed in the stabilization stage 3 phase, but that is already directly bound by ETV2 and epigenetically primed for expression at induction stage 1 (2D monolayers). ETV2 ChIP-sequencing was performed on R-VECs using an anti-flag antibody. Mouse IgG was used as a control for ETV2 ChIP. Histone modification ChIP for H3K4me3, H3K27ac and H3K27me3 was performed on both CTRL-EC and R-VEC at the induction stage 1 (2D monolayers). Enriched regions were analyzed by ChIP-sequencing. Black bar, ETV2 enriched regions. Green bar, the region with increased K4me3 modification. Blue bar, the region with increased K27ac modification. Promoter regions bound by ETV2 are highlighted in cream. Track range ETV2/K27me3/K27ac/, 0-0.3; K4me3/input/IgG, 0-1. For statistics see **Supplementary Data 2.** For media formulations refer to **Supplementary Data 3.**

Extended Figure 8. R-VEC arborize islet explants and organoids
a) Human islet explants were cultured in Matrigel droplets either with GFP labeled CTRL-EC or R-VEC (day 4). **b)** Insulin secretion fold change post glucose stimulation at 16.7 mM vs. 2mM glucose (2-week time point). **c)** Vessel area of ECs directly interacting with islets at week 2. **d)** EpCAM and VEcad staining of islets co-cultured in a Matrigel droplets at 2 weeks. **e)** Orthogonal projections of R-VECs in co-culture with human islets at two weeks. **f)** Human colon organoids (hCOs) were derived from isolated crypts from colon biopsies of healthy human donors. Colon organoids were confirmed to express proper markers by quantitative RT-PCR. **g)** Quantitative RT-PCR of various colon markers for

hCOs, co-cultured with CTRL-EC or co-cultured with R-VEC for 8 days. Epithelial cells were sorted out as live $CD31^{neg}$ cells. **h)** Mouse small intestine organoids were cultured alone, or in the presence of CTRL-EC of R-VEC (day 8). Confocal representative images of EdU^{+} (proliferating cells), $KRT20^{+}$ (differentiated epithelial cells in blue) ECs (mCherry - red) of co-culture experiment with mouse intestinal organoids. **i)** Quantification of vessel area over the course of 7 days in co-cultures of mouse intestine organoids with CTRL-EC or R-VEC. **j)** Vessel arborization quantified as EC sprouts in direct contact/organoid in CTRL-EC versus R-VEC wells. **k)** Time-lapse representative images show the progression of interacting ECs with tumor colon organoids. CTRL-EC (in green) fail to interact with tumor colon organoids (in red) (top panel), while R-VEC (in green) form robust EC tubes to tap and wrap tumor colon organoids (in red) (bottom panel). **l)** Orthogonal projections of colon tumor organoids co-cultured with R-VECs (day 8). Data are represented as mean±S.E.M. ns= not significant; *<0.05, **<0.01, and ***<0.001. For statistics see **Supplementary Data 2.** For media formulations refer to **Supplementary Data 3.**

Extended Figure 9. Endothelial and epithelial cell identification by single cell RNA-seq from co-cultures of normal colon organoids with R-VECs

a) Schematic of 10x Chromium single-cell RNA-seq experiments of R-VECs alone, R-VECs co-cultured with normal human colon organoids (hCO) or normal hCO alone. Samples were analyzed 7 days post co-culture. The same medium was used across all three conditions. **b)** UMAP of cells from each condition alone and the three conditions merged. **c)** Endothelial cells were identified as cells expressing either VEcad, PECAM1 or VEGFR2 and negative for the epithelial marker EpCAM. Epithelial cells were defined as $EpCAM^{+}$ and negative for any EC markers VEcad, PECAM1, or VEGFR2. **d)** UMAP of the 9 unique clusters identified in the merged samples. **e)** Endothelial and epithelial cell specific markers were used to confirm the EC clusters (clusters 1 to 7) vs. epithelial cell clusters (clusters 8 and 9). **f)** The identity of epithelial cells in clusters 8 and 9 was confirmed as colon-specific by expression of markers, including SATB2, CA4, CA2 and others. For statistics see **Supplementary Data 2.** For media formulations refer to **Supplementary Data 3.**

Extended Figure 10. Endothelial and epithelial cell identification by single cell RNA-seq from co-cultures of colon tumor organoids with R-VECs

Schematic of 10x Chromium single cell RNA-seq experiments of R-VECs alone, R-VECs co-cultured with human colorectal cancer organoids (hCRCO) or hCRCO alone. Samples were analyzed 7 days post co-culture. The same medium was used across all three conditions. **b)** UMAP of cells from each condition alone and the three conditions merged. **c)** Endothelial cells were identified as cells expressing either VEcad, CD31 or VEGFR2 and negative for the epithelial marker EpCAM. Epithelial cells were defined as $EpCAM^{+}$ and negative for any EC markers VEcad, CD31 or VEGFR2. **d)** UMAP of the 9

unique clusters identified in the merged samples. **e)** Endothelial and epithelial cell-specific markers were used to confirm the endothelial cell clusters (clusters 6,7,8) vs. epithelial cell clusters (clusters 1,2,3,4,5,9). **f)** UMAP of merged epithelial cell fractions from hCRCO cultured alone or co-cultured with R-VECs. Six unique clusters were identified. **g)** Heatmap and **h)** Dotplot of differentially expressed genes in tumor epithelial cells in cluster 2 and cluster 5 which are enriched upon co-culture with R-VECs. Differential expression was performed using the Wilcoxon rank-sum test FDR $p<0.05$. For statistics, see **Supplementary Data 2.** For media formulations refer to **Supplementary Data 3.**

Methods

Cell culture of endothelial cells (ECs)

The approval for procuring discarded left-over human umbilical vein endothelial cells (HUVEC) and human adipose tissue ECs were obtained through Weill Cornell Medicine investigational review board. The ECs were isolated in laboratory as previously described using the collagenase-based digestion approach[25,26]. The cells were then grown in tissue culture dishes coated with 0.2% gelatin in complete EC media. Complete EC media is composed of 400 ml of M199, 100 ml heat-inactivated FBS, 7.5 ml Hepes, 5 ml antibiotics (Thermo Fisher, 15070063), 5 ml glutamax (Thermo Fisher, 35050061), 5 ml of lipid mixture (Thermo Fisher, 11905031), and 25 mg endothelial cell (EC) growth supplement (Alpha Aesar, J64516-MF) (**Supplementary Data 3**). The cells were transduced with lenti-PGK-ETV2 or an empty lenti-vector at P1/P2. In some instances, the cells were also labeled by using PGK-mCherry or PGK-GFP lenti-virus. The cells were split 1:2 using accutase and passaged on gelatinized plates. As needed, cells in 2D (stage 1 induction) were frozen down to be used in future experiments. All comparisons for all assays and co-cultures were performed using the same parental EC line with and without ETV2. Overall, HUVECs from more than 10 different isolations were used for the experiments. Cells used for tube formation assays were of passage 5-10.

Human adipose-derived ECs were isolated by mechanical fragmentation followed by collagenase digestion for 30 minutes. After plating the crude population of cells on the plastic dish and expansion for 5 to 7 days, the cells were then sorted to purify VEcadherin^{+}CD31^{+} ECs and expanded as described above. Human adipose ECs were cultured in the same media described above for HUVECs. At least three different isolations of adipose ECs were used in our experiments. Human microvascular cardiac (PromoCell, C12286), aortic (PromoCell, C12272), Pulmonary (PromoCell, C-12282) and microvascular dermal (PromoCell, C12265) ECs were acquired from Promocell and cultured in EC growth medium MV (PromoCell, C22020).

Lentiviral transduction of ECs

ECs were transduced with ETV2 lenti-particles or empty vector lenti-particles. ETV2 cDNA [NM_014209.3] was introduced into the pCCL-PGK lentivirus vector [Genecopeia]. For purposes of ChIP analysis, a triple Flag-tag was subcloned in the ETV2 construct at the amino terminus[27]. After 1 week of transduction, ECs were collected for mRNA isolation and qRT-PCR analysis. The relative ETV2 RNA unit was determined by calculating the relative ETV2 mRNA expression compared to GAPDH using the following formula: $((2^{\wedge -(Ct(ETV2)-Ct(GAPDH))}) * 1000)$ (Primers found in the Extended table 3). Cells with relative ETV2 RNA unit within the range of 60-100 were used for all experiments. An MOI of 3 gave us relative expression levels of 60-80 as calculated by mRNA expression. MOI was calculated by converting particles of P24 to IFU and then to MOI based on cell number (kit: Katara, 632200). MOI of 3 was also found to be adequate for Cardiac and Aortic ECs. An MOI of 6 was instead required for adipose and dermal ECs. Polybrene at 2 μg/ml was utilized for all transductions. ETS1, *myr*AKT, mCherry, GFP, were also introduced into the pCCL-PGK lentivirus vector and an MOI of 3 was used for all transductions.

For inducible expression of ETV2, ECs were transduced with doxycycline-inducible ETV2 lenti-viruses (pLV[Exp]-Puro-TRE>hETV2 [NM_014209.3], VectorBuilder VB170514-1062dfs and pLV[Exp]-Neo-CMV>tTS/rtTA_M2, VectorBuilder VB160419-1020mes) where presence of doxycycline turns on ETV2 expression. Post 1 week doxycycline (1 μg/ml) induction of ETV2, cells were collected to determine the relative ETV2 mRNA unit. Cells with relative ETV2 RNA unit within 60-100 were used for all experiments. An MOI of 50 was required for the inducible ETV2 lentiviral particles and rtTA lentiviral particles.

Lentivirus production

All lentiviral plasmids were prepared with a DNA Midiprep kit (Qiagen, 12145). Viruses were packaged in 293T cells by co-transduction with 2nd- or 3rd-generation of packaging plasmids. Culture media were collected 48hrs post-transduction and virus particles concentrated using a Lenti-X concentrator (Katara, 631232), resuspended in PBS without calcium/magnesium (Corning, 21040CV), and stored at -80°C in small aliquots. Virus titers were determined with a Lenti-X p24 titer kit (Katara, 632200).

Tube formation assays

Twenty-four well plates were coated with 300 μl of Matrigel (Corning) for 30 min in 37°C incubator. Meanwhile, cells with or without ETV2 were accutased and counted. Cells were then resuspended in StemSpan (Stem Cell Technologies) supplemented with 10% knock out serum (Thermo Fisher, 10828028) and cytokines: 10ng/ml FGF (Peprotech, 1000-18B), 10ng/ml IGF1 (Peprotech, 100-11), 20ng/ml EGF (Peprotech, AF-100-15), 20 ng/ml SCF (Peprotech, 300-07), 10 ng/ml IL6 (Peprotech, 200-06). One hundred thousand cells either with or without ETV2 were then dispersed in each well in 1 ml of media. Cultures were placed in a 37°C incubator with 5% oxygen for the remainder of tube formation experiments.

Media was changed every other day, by replacing 750 µl of media with fresh media. Care was taken to not disrupt the tubes during all media changes. For several occasions, a mixture of defined matrices comprised of Laminin, Entactin mixture (Corning, 354259) and Collagen IV (Corning, 354245) (L.E.C) was used instead of Matrigel as indicated in the text. We combined these defined matrices at different ratios among Laminin, Entactin and Collagen IV components and ultimately found the most effective combination of these gel mixtures for tube formation assays, which was comprised of 200 µl of (Concentrations slightly vary for each lot #, always diluted to 16.5mg/ml in PBS first) Laminin, Entactin and 100 µl of Collagen IV (Concentrations slightly vary for each lot#, first diluted to 0.6 mg/ml in PBS) mixed together on the ice and stored at 4^{o}C overnight before usage. The final format of L.E.C. consisted of 11 mg/ml Laminin, Entactin mixture and 0.2 mg/ml Collagen IV. The volume of L.E.C was increased as needed, as long as the ratios/final concentrations were maintained. Vessel area was measured over the course of 24 hrs to 12 weeks for stage 2 Remodeling and stage 3 Stabilization phases. EVOS inverted microscope was used to capture images in their different/randomized places in each well for each condition and time point with a 4x objective. All the images were then analyzed for the lumenized vessel area using ImageJ to trace the vessel area. The same procedure was used for cells transduced with ETS1 or *myr*AKT1[28] or K-RAS [26] transduced ECs.

Tube formation assay in different media formulations

ECs were accutased and plated on Matrigel at 100,000 cells/well of 24-well plates as described above. To assess the tube formation assays of ETV2 ECs vs Control ECs, we compared their capabilities to form a tubular network in 3 different medium formulations: StemSpan tube formation media (**Supplementary Data 3**) the serum-free medium containing StemSpan supplemented with knockout serum and cytokines (Stem Span- (Stem Cell Technologies) supplemented with 10% knock out serum (Thermo Fisher, 10828028) and cytokines: 10ng/ml FGF (Peprotech, 1000-18B), 10ng/ml IGF1 (Peprotech, 100-11), 20ng/ml EGF (Peprotech, AF-100-15), 20 ng/ml SCF (Peprotech, 300-07), 10 ng/ml IL6 (Peprotech, 200-06)). Medium formulation 2 (EGM2) is a commercialized EC growth medium (**Supplementary Data 3**) (PromoCell, C22111). Medium formulation 3 (MF3) is the complete EC medium (**Supplementary Data 3**) with serum that was used to maintain and propagate ECs (400 ml of M199, 100 ml heat-inactivated FBS, 7.5 ml Hepes, 5 ml antibiotics (Thermo Fisher, 15070063), 5 ml glutamax (Thermo Fisher, 35050061), 5 ml of lipid mixture (Thermo Fisher, 11905031), and 25 mg endothelial cell growth supplement (Alpha Aesar, J64516-MF). Media were changed every other day. Images were acquired at different time points. ImageJ was utilized to measure vessel area over time.

Video set up for HUVECs cultured in 3D matrices in different medium formulations

GFP-labeled control HUVECs and R-VECs were embedded inside L.E.C at 5 million cells/ml. Gels were polymerized on glass-bottom culture dishes at 37^{o}C incubator for 15mins. Subsequently, either a

commercialized EC growth media (EGM-2) or StemSpan tube formation media (**Supplementary Data 3**) serum-free medium containing StemSpan supplemented with knockout serum and cytokines was added into the cell culture as described above. The medium was also supplemented with Trolox, Vitamin E analog (6-hydroxy-2,5,7,8-tetramethylchroman-2-Carboxylic Acid) (Sigma) at 100μM to enable long-term imaging. The cultures were mounted on temperature- and gas- controlled chamber for live-cell imaging. Time-lapse videos were acquired with a Zeiss Cell Observer confocal spinning disk microscope (Zeiss) equipped with a Photometrics Evolve 512 EMCCD camera at an interval of 40 mins over 3 days. The media was refreshed every 2 days.

Immunofluorescent staining of tubes *in vitro*

At 8 to 12 weeks all media was removed from the wells. The tubes were washed once with PBS and fixed for 30 min in 4% PFA at room temperature. Then the wells were rewashed with PBS and put in blocking buffer (containing 0.1% Triton-X) for 1 hr at room temperature. For proliferation studies, a 16-hour pulse of EdU (Click-iT EdU kit, Thermofisher scientific C10337) was used for all three stages of vessel formation.

Electron microscopy

Tissues were washed with serum-free media or PBS then, fixed with a modified Karmovsky's fix of 2.5% glutaraldehyde, 4% paraformaldehyde and 0.02% picric acid in 0.1M sodium cacodylate buffer at pH 7.2. Following a secondary fixation in 1% osmium tetroxide, 1.5% potassium ferricyanide samples were dehydrated through a graded ethanol series, and embedded in an Epon analog resin. Ultrathin sections were cut using a Diatome diamond knife (Diatome, USA, Hatfield, PA) on a Leica Ultracut S ultramicrotome (Leica, Vienna, Austria). Sections were collected on copper grids and further contrasted with lead and viewed on a JEM 1400 electron microscope (JEOL, USA, Inc., Peabody, MA) operated at 100 kV. Images were recorded with a Veleta 2K x2K digital camera (Olympus-SIS, Germany).

Atomic Force Microscopy (AFM) Measurements

AFM was used to examine the stiffness of HUVECs and adult human adipose ECs. Brightfield images of cells, for determination of the location of stiffness measurements, were acquired using an inverted microscope (Zeiss Axio Observer Z1) as the AFM base (20x 0.8 NA objective). An MFP-3D-BIO Atomic Force Microscope (Asylum Research) was used to collect force maps. A 5 μm borosilicate glass beaded probe (Novascan) with a nominal spring constant of 0.12 N/m was used for all measurements. Each force map sampled a 60 μm x 60 μm region, in a 20 x 20 grid of force curves (400 force curves total) under fluid conditions which covered an area of 360 μm^2. The trigged point was set to 2 nN with an approach velocity of 5 μm/sec. The force-indentation curves were fit to the Hertz model for spherical tips utilizing the Asylum Research Software to determine Young's modulus, with an assumed Poisson's ratio value of 0.45 for the

sample. Force maps of stiffness along with individual stiffness values for each measured point were then exported from the Asylum Research Software for further analysis. A custom-made MATLAB (MathWorks) script was written to correctly analyze the data for the stiffness of the cells and filter measurements such that only data 1 μm from the glass bottom dish was analyzed (to remove any substrate effect from the measurements).

RNA and protein collection from endothelial tubular capillaries

At indicated time points, capillaries of ECs from tube formation assays were collected for RNA sequencing and Western blotting. Before the cells were collected, the media was completely removed from the well. 2ml of 2 mg/ml Dispase (Roche 38621000) was added into each well to dissociate the EC tubes for 45 mins at 37^{o}C with gentle shaking. Dissociated cells were pelleted, washed once in PBS and subsequently collected for either mRNA or protein isolation. On several occasions, dissociated ECs from tubes were pooled from multiple wells of the same EC line and experiment to allow sufficient isolation of mRNA and protein for downstream analysis.

Western immunoblot

Cells were lysed into 1X SDS loading buffer (50 mM Tris-HCl pH 6.8, 5% beta-mercaptoethanol, 2% SDS, 0.01% bromophenol blue, 10% glycerol) followed by sonication (Bioruptor, 2X 30 seconds at high setting). Proteins were solved on 5-15% gradient Tris-glycine SDS-PAGE and semi-dry transferred to nitrocellulose membranes. The following primary antibodies were used at indicated dilutions: Rap1 (CST, #2399, 1:1,000); RASGRP3 (CST, #3334, 1:1,000), GAPDH (CST, #5174, 1:10,000); AKT (CST, 34685, 1:5,000); p-S473-Akt (CST, #4060, 1:2,000); ETS1 (CST, #14069, 1,000); and ETV2 (Abcam, ab181847, 1:1,000) (Extended Table 1). HRP-conjugated secondary antibodies and the ECL Prime Western Blotting System (GE Healthcare, RPN2232) were then used. Chemiluminescent signals were captured with a digital camera (Kindle Biosciences) and images of protein bands taken for quantification using ImageJ.

***In vivo* experiments**

All animal experiments were performed under the approval of Weill Cornell Medicine Institutional Animal Care and Use Committee (IACUC), New York, NY. HUVECs transduced with an empty vector or ETV2, and labeled with GFP or mCherry (2 million cells/plug) were injected subcutaneously in male or female 8-12 week old SCID-beige mice (Taconic). The cells were first resuspended in PBS (50 µl) and then mixed with Matrigel (Corning, 356237) or L.E.C. mixture as described above to a final volume of 350 µl. The gels were also supplied with FGF2 (10ng/ml) (Peprotech, 1000-18B), VEGF-A (20ng/ml) (Peprotech, 100-20), and heparin (100µg/ml) (Sigma H3149-100KU). Each mouse received two plugs: one with control cells and the other with cells transduced with ETV2. Mice implanted with plugs were injected retro-orbitally with anti-

human VEcad (clone BV9- Biolegend) conjugated to Alexa-647 (25 µg in 100 µl of PBS) or 70kDa fluorescently labeled lysine fixable dextran (ThermoFisher) and sacrificed 8 min post-injection. Whole-mount images were taken directly on the confocal microscope Zeiss 710 using a well containing a coverslip bottom. The plugs were fixed in 4% PFA overnight and then dehydrated in ethanol or put in sucrose for further immunostaining. The dehydrated plugs were sent to Histoserv Inc. for further processing, sectioning and H&E, Picrosirius, or Masson staining. The sections were processed for immunostaining as described below. GFP labeled K-RAS cells were injected in mice as described above, but due to a rapid increase in size mice bearing K-RAS plugs were harvested at 2 weeks.

Immunostaining of sections

OCT frozen sections (20 µm), previously fixed in 4% PFA and treated in sucrose, were washed once with PBS. Then, the slides were incubated in blocking buffer (0.1% Triton-X, 5% normal donkey serum, 0.1% BSA), for 30 minutes at room temperature and overnight in primary antibodies at appropriate dilution listed in Extended Table 1 at 4°C in blocking buffer. For thicker sections (50 µm) tissues were blocked overnight in blocking buffer 4°C (0.3% Triton-X, 5% normal donkey serum, 0.1% BSA) and then for two days in primary antibody in blocking buffer at 4°C (0.3% Triton-X, 5% normal donkey serum, 0.1% BSA). The next day, the slides were washed 3x for 10 min at room temperature and then incubated for three hours in fluorescently conjugated secondary antibodies (1:1000). Finally, the slides were washed 3x for 10 minutes and counter stained with DAPI. The sections were mounted on coverslips. Zeiss 710 confocal or Zeiss Cell Observer confocal spinning disk microscope (Zeiss) was utilized to acquire images. For stroma staining, a mouse anti-PDGFRβ antibody (1:500, Biolegend) or an anti-mouse SMA (1:200, Abcam) were used. Mouse ECs were counterstained with mouse anti-endomucin antibody (1:100, Santa Cruz). (Several images were taken from sections from different layers of each plug. At least 12 pictures (4/mouse) from different slides were taken for each condition and time point. Images were processed using ImageJ and the percentage of vessel area over the area of each image field was quantified by using the threshold feature in ImageJ.

Rap1 pull down and Western Blots

A 10-cm plate of either HUVECs or ETV2-transduced HUVECs (flat-2D induction stage) was used for the active Rap1 assay (Cell Signaling, 8818S) according to the manufacturer's guidelines for the kit. Briefly, the cells were washed once with PBS and then starved for three hours in M199 medium with 0.5%BSA. The cells were then scraped in the lysis buffer supplied with the kit and resuspended at ~1 mg/ml. A fraction was saved as input and the rest of the cells were used for Rap1-GTP pull-down. Positive and negative controls, as well as beads only control, were performed according to the manufacturer's guidelines. Proteins were solved on 5-15% gradient Tris-glycine SDS-PAGE and semi-dry transferred to nitrocellulose membranes. The membranes were then blocked in 5% milk in PBST and incubated in the provided Rap1 (1:1000)

antibody, GAPDH and/or ETV2 antibody for 48 hours. After 48 hours, the membranes were washed 3x for 5 min and incubated in HRP conjugated secondary antibody. Finally, upon secondary washings, the membrane was blotted in ECL and chemiluminescent signals captured with a digital camera (Kindle Biosciences) and images of proteins bands were taken for densitometric quantification using ImageJ.

Rap1 inhibition experiment

Tube formation assays for ECs with or without ETV2 were set up in 24 wells as described above. The next day, Rap1 inhibitor (GGTI-298, Tocris) resuspended in DMSO was added to the wells at a 1:1000 dilution at the final concentration of 10μM, while the same amount of DMSO was added to the control wells. The inhibitor and media were changed every other day for 4 weeks. Images were obtained and vessel area calculated as described above at 1-week and 4-week time points.

RASGRP3 knockdown experiments

shERWOOD-UltramiR RASGRP3 shRNA lentiviral constructs (in pZIP-TRE3G) were purchased from TransOMIC Technologies. The clone# and targeted RASGRP3 sequences are as follows: ULTRA-3265848, AAGGGCAGAAGTCATCACAAA ;ULTRA-3265850, CCTTGGAGTACACTTGAAAGA. The control shRNA (ULTRA-NT, ATGCTTTGCATACTTCTGCCT) targets a fly luciferase RNA sequence. Lentivirus was prepared as described above, using 2nd generation packaging plasmids. R-VECs (stage 1) were transduced with either shRNA virus or control shRNA virus (MOI=3). Doxycycline was added at day 1 of the remodeling stage (stage 2) and media with doxycycline was replaced every other day for 4 weeks. Images were obtained and vessel area calculated and described above at 2 and 4-week time points. To confirm RASGRP3 knockdown, doxycycline was added in stage 1 R-VEC cells for 1 week and then the cells were collected for Western Blot analysis.

Proteasome inhibition experiment

R-VEC vessels were prepared on Matrigel as described above. At the stabilization stage (4 weeks), R-VEC tubes were treated with either 20μM of MG132 (Selleck Chemicals) or DMSO for 6hrs. The media was removed and the wells were washed once with PBS. R-VEC tubes were then incubated in a solution of 2mg/ml Dispase (Roche) for 45 minutes at 37^{o}C to dissociate the tubes. 20μM of MG132 (Selleck Chemicals) or DMSO was continuously provided during the dissociation period. Dissociated cells were collected and further processed for Western blotting as described above.

Isolation of ECs from ETV2 reporter mice

ETV2-Venus reporter mice were a kind gift of Dr. Valerie Kouskoff [29]. Briefly, embryos were isolated at E9.5 from pooled litters of ETV2-Venus reporter mice. For each independent biological replicate, five litters of

mice at E9.5 were pooled together. All embryos were accutased for 20 min at 37°C and then triturated several times with a pipette. The cells were post-stained for anti-mouse CD31 and anti-mouse CD45 antibodies, and then sorted as either ETV2Venus^{+}, CD31^{+}, CD45^{-} or as CD31^{+}, CD45^{-} (ARIAII, BD). Cells were sorted straight into Trizol-LS and RNA further purified using Qiagen RNA-easy isolation kit.

Intestinal Tissue Harvesting and Decellularization

Intestines were harvested from Sprague Dawley rats ranging 250-350g in weight. Briefly, under aseptic conditions a midline laparotomy was performed and the intestine exposed. A 5 cm long intestine segment was isolated, preserving the mesenteric artery and the mesenteric vein that perfuse the isolated segment. Both vessels were cannulated with a 26G cannula, and intestinal lumen was cannulated using 1/4" barbed connectors. The isolated segments were decellularized providing perfusion through vasculature and lumen at 1ml/min using a peristaltic pump (iPump). Decellularization process consisted of Milli-Q water for 24h, sodium deoxycholate (Sigma) for 4h and DNAse I (Sigma) for 3h. Decellularized intestines were sterilized with gamma radiation before use.

Bioreactor culture

Decellularized intestines were seeded either with 5 million GFP^{+}ETV2^{+} human ECs or with 5 million GFP^{+} Control-ECs (CTRL-ECs). Cells were seeded through the mesenteric artery and mesenteric vein. Seeded intestines were mounted inside a custom-made bioreactor under sterile conditions. After 24h, perfusion was started through the mesenteric artery at 1ml/min using a peristaltic pump (iPump). Cells were grown in complete EC media: M199/EBSS (HyClone, SH302503.01) supplemented with 20% Heat inactivated FBS, 1% Pen-Strep, 1.5 % HEPES (Corning 25-060-CI), 1% Glutamax (Gibco 35050-061), 1% Lipid mixture (Gibco 11905-031), 1% Heparin (Sigma H3149-100KU) and 15ug/ml Endothelial Cell Growth Supplement (Merck 324845) for the first 5 days, then cells were grown for 2 days in Stemspan (Stemcell Technologies) supplemented with 10% knock out serum (Thermo 10828028), 1% Pen-Strep, 1% Glutatamax, 10ng/ml FGF2 (Peprotech 1000 18B), 20 ng/ml EGF (Invitrogen PHG0311), 10ng/ml IGF2 (Peprotech 100-12), 20ng/ml SCF (Peprotech 300-07) and 10ng/ml IL6 (Peprotech 200-06). After 7 days, re-endothelialized intestines were harvested under sterile conditions and segments 5x7mm were excised for heterotopic implantation. Remaining intestinal tissue was then fixed in 4% paraformaldehyde, mounted and prepared for imaging by fluorescent microscopy. To assess the patency of the vessels, some re-endothelialized intestines were perfused with fluorescently-labeled LDL.

Heterotopic graft implantation

Animals used for these studies were maintained and experiments performed in accordance with the UK Animals (Scientific Procedures) Act 1986 and approved by the University College London Biological

Services Ethical Review Process (PPL 70/7622). Animal husbandry at UCL Biological Services was in accordance with the UK Home Office Certificate of Designation. NOD-SCID-gamma (NSG) mice, aged between 8 and 12 weeks, were anesthetized with a 2-5% isoflurane-oxygen gas mix for induction and maintenance. Buprenorphine 0.1 mg/Kg was administered at the induction of analgesia. Under aseptic conditions a midline laparotomy was performed. The stomach was externalized from the incision and the omentum stretched from the great curvature. A segment of the engineered intestine was then enveloped in the omentum, using 8/0 Prolene suture to secure the closure of the omental wrap. The stomach and the omentum were placed back in the abdomen and the laparotomy closed using 6/0 Vicryil suture. Animals were allowed to normally eat and drink immediately after surgery and no further medications were administered during the post-operative periods. After 1 week or 4 weeks, the mice were intravenously injected with fluorescently-labeled anti-human VEcad (hVEcad) (BV9 Biolegend) as described earlier, then euthanized. Grafts were retrieved together with the omental envelope and fixed in 4% paraformaldehyde, mounted and prepared for imaging by fluorescent microscopy.

Analysis of vascular parameters for decellularized intestine experiments

Images for *in vitro* EC revascularization were processed using ImageJ by setting a threshold and quantifying the area covered by the CD31 signal with respect to the intestine area. *In vivo* quantification of cells positive for GFP and VEcadherin was performed on images acquired with a confocal microscope (Zeiss LSM710) and evaluation of vascular parameters was performed using Angiotool software (National Cancer Institute)[30].

Quantification of proliferating cells and apoptotic cells in decellularized scaffolds

Explanted intestinal grafts were fixed in 4% PFA, embedded in OCT and sectioned. Sections were stained for Cleaved-Caspase3 (Cell Signaling, 9661S) and for Ki67 (Abcam, AB15580). First, the sections were blocked for 1 hour in PBS with 10% donkey serum. Then, primary antibodies were incubated overnight at 4°C in blocking solution with the addition of 0.5% Triton-X. Primary antibodies were washed 3 times with PBS before the secondary antibody was added. Secondary antibody for donkey anti-mouse or rabbit (Alexa Fluor 547 or 647; Life Tech) was used at a dilution of 1:500 in blocking solution with 0.5% Triton X-100 and incubated at room temperature for 1 hour. Secondary antibody buffer was washed off with PBS 3 times and the slides mounted in a solution containing DAPI. Images were acquired with a confocal microscope (Zeiss LSM710). Three fields of view (425.10 µm x 425.10 µm in size) were evaluated per animal and the ratio between human VEcadherin (injected intra-vitally before sacrifice) and Cleaved-Caspase3 or Ki67 positive cells quantified.

Primary human pancreatic islets in static co-culture with ECs

Primary human islets were purchased from Prodo Laboratories Inc, California. Twenty-five human islets were either cultured alone, co-cultured with CTRL-ECs, or co-cultured with R-VECs. CTRL-ECs and R-VECs were used at 5 million cells/ml. The human islets with and without ECs were mixed in 40μL of Matrigel and plated into wells of Nunc IVF 4-well dish (Thermo Scientific, cat# 144444). Islets and ECs were co-cultured with serum free islet medium (SFIM, **Supplementary Data 3**). The medium was comprised of glucose-free RPMI 1640 and supplemented with 0.1% human serum albumin, 10μg/ml human transferrin, 50μM Ethanolamine, 50μM Phosphoethanolamine, 6.7μg/ml sodium selenite, 10ng/ml bFGF (FGF2), 100μg/ml heparin, and 5.5mM Glucose. After two weeks of co-culture, samples were prepared for glucose stimulated insulin secretion (GSIS). Samples were starved in Krebs-Ringer bicarbonate HEPES (KRBH) buffer containing 2mM glucose for 2hrs, followed by 45min in 2mM glucose as the basal insulin secretion and 45min in 16.7mM glucose as the stimulated insulin secretion. Insulin concentrations at the end of basal and stimulated phases were determined using STELLUX Chemi human Insulin ELISA (ALPCO). For each group, there were 11 replicates, with islets derived from 4 different donors. In other experiments, 200 human islets were cultured alone or mixed with 250,000 CTRL-ECs or 250,000 R-VECs in 50μl Matrigel droplets. Human islet explants in co-culture were stained for EpCAM and VEcad and imaged at 1 and 2 weeks. Briefly, the growth media was removed and the cells were fixed in 4% PFA for 20 minutes. They were then permeabilized in 0.5% Triton-X for 20 minutes and blocked in IF Buffer (PBS, 0.2% Triton-X, 0.05% Tween, 1% BSA) for 1 hour. Then the cells were incubated in primary antibodies overnight in IF buffer: anti-EpCAM (1:100, Biolegend), VEcad (1:100, R&D&. They were then washed 3 times with PBS 0.1% Tween. The wells were then incubated with secondary antibodies (1:1000) in the IF buffer for 3 hours. The solution was removed and DAPI in PBS was added for 5 minutes and washed twice with PBS 0.1% Tween.

To quantify the interacting vessels with human pancreatic islets, co-cultures were imaged using a 10x objective to capture both GFP-labeled vessels and human pancreatic islets in the bright field. Using the custom MATLAB code, we traced the area of GFP-labeled vessels that surrounded and wrapped the human pancreatic islets for both co-cultures with CTRL-ECs and with R-VECs.

Vascular network formation in microfluidic devices

We manufactured a more substantial scale device using photo-lithography as previously described[17]. The distance between the two fluidic channels or the width of the device is 3mm (increased from 1mm). The length of the device or the length of the fluidic channels is 5mm long. The height of the device is 1mm high. The total volume of the device is 15 microliters. Briefly, each device is comprised of two layers of poly(dimethylsiloxane) (PDMS; Sylgard 184; Dow-Corning), which are cast from silicon wafer masters. The devices are plasma-treated with plasma etcher (Plasma Etch) and subsequently treated with (3-

Glycidyloxypropyl) trimethoxysilane (Sigma, 440167) overnight. The next day, they are submerged in water to wash overnight before usage. All devices are kept in 37°C incubator with 20% oxygen.

A mixture of 3 million/ml ETV2 HUVECs or control HUVECs in 5mg/ml bovine Fibrinogen (Sigma) and 3U/ml bovine thrombin (Sigma) was injected into the devices with two 400μm acupuncture needles (Hwato). After the cell and gel mixture polymerized, the acupuncture needles were pulled out leaving two hollow channels. HUVECs were seeded into the hollow channels to form two-parent vessels on the next day. The devices were placed on a platform rocker for the entire experiment (Benchmark). Cells were cultured in the medium for vessel formation in microfluidic devices (**Supplementary Data 3**) and refreshed daily until day 7, when the devices were fixed and imaged.

For human pancreatic islet culture experiments, devices were also set up similar to experiments with ECs alone. Approximately 75 human pancreatic islets were mixed either alone or with CTRL-EC or R-VECs (4 million cells/ml) cells in 5mg/ml bovine fibrinogen and 3U/ml bovine thrombin to a total volume of 30μL and injected into the devices. The needles were removed after fibrin gel polymerization, and 200μL of medium for human pancreatic islet co-culture medium (**Supplementary Data 3**) was added into each of the fluidic channels. The devices were placed on a platform rocker (Benchmark 2000) during the entire experiment.

Glucose stimulation insulin secretion (GSIS) assay for human pancreatic islets in the devices.

Human pancreatic islets were placed in the devices as described above either alone, or in co-culture with CTRL-ECs or R-VECs. Human cadaveric islets (from Prodo Labs, California) were procured from three healthy separate donors, with a total of n=4 devices for No-EC, n=4 devices for CTRL-EC, n=8 devices for R-VEC. After 4 days, the media was removed in all the devices. The devices were then starved with 2 mM glucose for 2 hours in the incubator. At the end of starvation, 300μL of 2 mM glucose KRBH buffer was added at the inlet of the device, and devices were incubated at 37°C for 3 minutes. Driven by gravity, KRBH buffer perfused through to the other side (outlet) of the device during the incubation. After the 3-minute incubation, fluid from the outlets was collected for insulin measurement through ELISA. The inlets were also emptied of any remaining fluid. Then, another 300 μL KRBH buffer was added to inlets, leaving the outlets empty. In R-VEC co-culture devices, 30 – 150 μL fluid was collected in the outlets due to high perfusion rates. In islets alone and CTRL-EC co-culture devices, only a small amount of fluid (<10 μL) was found in the outlets. To enable sample collection, we rinsed the outlets of islets alone and CTRL-ECs co-culture devices with 150 μL KRBH buffer and collected all outlet liquid for insulin measurement by using ELISA. Such sample collection was repeated for a total of 8 times using 2 mM glucose KRBH buffer, and another 8 times using 16.7 mM glucose KRBH buffer. In the end, we acquired a series of semi-dynamic GSIS samples. We examined the insulin concentration at the outlet of the device at the 3rd (at t=9 min) and 8th (t=24 min) collections at both 2 mM and 16.7 mM glucose phases. The insulin level per device was

calculated as: insulin per device = insulin concentration × collected volume. Basal insulin levels were determined as the average of the 3rd and 8th collections at 2 mM glucose. Insulin concentration was determined using STELLUX Chemi human Insulin ELISA (ALPCO).

Staining protocol for experiments in devices.

To stain for ECs in the devices, right before the experiment was terminated, all medium was aspirated in both fluidic channels in the devices. 200µL VEcadherin antibody conjugated with Alexa 647 at 10µg/ml (Biolegend) was placed on one of the fluidic channels and allowed to slowly perfuse through the lumenized R-VEC vessels for 15-20 mins in the incubator from one fluidic channel to the other fluidic channel. The device was then washed 3x with basal medium and fixed with PFA for 45mins.

When co-culture experiments were set up with human pancreatic islets, the same protocol was utilized to stain for R-VEC lumenized vessels with VE-cadherin conjugated antibody. Post-fixation, the device was permeabilized with 0.1% Triton-X for 45 mins and further stained with either EpCAM for human colon organoids or human pancreatic islets. To stain for EpCAM (Biolegend) the conjugated antibodies were added to both fluidic channels at 10µg/ml for 48 hrs on a rocker at 4^{o}C. The devices were washed 3x with 1xPBS and subsequently washed and submerged into 1xPBS for 24 hrs on a rocker at 4^{o}C. A similar staining procedure was used for insulin and post-VEcadherin staining, except permeabilization was carried out overnight, followed by primary antibody staining as described above and secondary staining for 24 hrs on a rocker at 4^{o}C. The devices went through washing for another 24 hrs with 1xPBS on a rocker at 4 ^{o}C and then imaged using a Zeiss 710 confocal.

Whole blood perfusion in vascularized microfluidic devices

For blood perfusion videos, vessels were prepared with 3 million/ml R-VEC cells, as described above. 400µL medium (Promocell) was refreshed. On day 7, blood was collected from a donor following IRB protocol in a heparinized tube. We sealed one end of both of the fluidic channels leaving two reservoirs diagonal to one another open for perfusion experiment. Whole heparinized human peripheral blood was obtained from consented healthy subjects with phlebotomy. Immediately, 200 microliters of whole blood were pipetted into one of the fluidic channels at the open reservoir, the blood cells along with intact plasma entered the fluidic channel, traversed through the lumenized R-VEC vessels and exited to the reservoir diagonal to the reservoir where blood entered. In experiments to perfuse blood in devices with R-VECs in co-culture with human pancreatic islets, we stained blood cells with Pkh26 Red fluorescent dye (Sigma, MMIDI26-1KT) according to the manufacturer protocol for 5 mins on ice. Fluorescently-labeled blood cells were pipetted into the reservoir, traversed through the lumenized R-VEC vessels, and exited to the diagonal reservoir. In other devices (CTRL-ECs + human pancreatic islets, and human pancreatic islets alone), fluorescently labeled blood cells were not able to traverse from one fluidic channel to the other fluidic

channel. Images were taken with Axio Observer Z1 equipped with Hamamatsu Flash 4.0 v2, sCMOS camera and 10x/0.45 objective.

Isolation and culture of mouse small intestine organoids

Mouse small intestine organoids were isolated as previously described[31]. Fifteen cm of the proximal small intestine was removed and flushed with cold PBS. After opening longitudinally, it was washed in cold PBS until the supernatant was clear. The intestine was then cut into 5 mm pieces and placed into 10 ml cold 5mM EDTA-PBS and vigorously resuspended using a 10ml pipette. The supernatant was aspirated and replaced with 10 ml EDTA and placed at 4ºC on a benchtop roller for 10 minutes. This was then repeated for a second time for 30 minutes. The supernatant was aspirated and then 10 ml of cold PBS was added to the intestine and resuspended with a 10 ml pipette. After collecting this 10 ml fraction of PBS containing crypts, this was repeated and each successive fraction was collected and examined underneath the microscope for the presence of intact intestinal crypts and lack of villi. The 10 ml fraction was then mixed with 10ml DMEM Basal Media (Advanced DMEM F/12 containing Pen/Strep, Glutamine, HEPES (10mM), 1mM N-Acetylcysteine (Sigma Aldrich A9165-SG) containing 10 U/ml DNAse I (Roche, 04716728001), and filtered through a 100µm filter into a BSA (1%) coated tube. It was then filtered through a 70µm filter into a BSA (1%) coated tube and spun at 1200 RPM for 3 minutes. The supernatant was aspirated and the cell pellet mixed with 5ml Basal Media containing 5% FBS and centrifuged at 200 g for 5 minutes. The purified crypts were then resuspended in basal media and mixed 1:10 with Growth Factor Reduced Matrigel (Corning, 354230). 40µl of the resuspension fluid was plated in a 48 well plate and allowed to polymerize. Mouse small intestine organoid growth media (Basal Media containing 40 ng/mL EGF (Invitrogen PMG8043), 100ng/ml Noggin (Peprotech 250-38), and 500 ng/mL R-spondin (R&D Systems, 3474-RS-050) were then laid on top of the Matrigel. In some experiments, small intestinal organoid growth media was made with R-spondin1 from conditioned media, collected from HEK293 cell lines expressing recombinant R-spondin1 (kindly provided by Calvin Kuo).

Maintenance of mouse small intestine organoids

Media was changed on organoids every two days and they were passaged 1:4 every 5-7 days. To passage, the growth media was removed and the Matrigel was resuspended in cold PBS and transferred to a 15ml falcon tube. The organoids were mechanically disassociated using a p1000 or a p200 pipette and pipetting 50-100 times. Seven ml of cold PBS was added to the tube and pipetted 20 times to fully wash the cells. The cells were then centrifuged at 1000 RPM for 5 minutes and the supernatant was aspirated. They were then resuspended in GFR Matrigel and replated as above. For freezing, after spinning the cells were resuspended in Basal Media containing 10% FBS and 10% DMSO and stored in liquid nitrogen indefinitely.

Mouse small intestine organoid co-culture and staining

Mouse small intestine organoids were co-cultured for 4-7 days either alone, or with CTRL-EC, or R-VEC and 5 million cell/ml of Matrigel final concentration. Organoids were mechanically dissociated as described above and mixed with the ECs, spun down and resuspended in GFR Matrigel. The mixture was then dispersed in 30µl droplets in 8-well chamber slides (Lab-Tek II, 154534) or 50µl droplets in Nunc IVF 4-well dish (Thermo Scientific, cat#144444). Cells were cultured in mouse small intestine organoid medium (**Supplementary Data 3**) Media compromised of mouse small intestinal media as described above (EGF 40ng/ml, Noggin 50 ng/ml, R-Spondin1 conditioned media (10%) + FGF-2 (10ng/ml) (Peprotech, 1000-18B) and heparin (100µg/ml) (Sigma H3149-100KU). Vessel area was quantified by the threshold function in ImageJ and individual sprouts in contact with the mouse small intestine organoids were counted and reported as vessel sprouts/organoids. Where indicated, 10 µM EdU was added to the growth media for 6 hours before fixing. The growth media was removed and the cells were fixed in 4% PFA for 20 minutes. They were then permeabilized in 0.5% Triton-X for 20 minutes and blocked in IF Buffer (PBS, 0.2% Triton-X, 0.05% Tween, 1% BSA) for 1 hour or immediately processed for EdU staining according to directions provided with the Click-iT Edu Imaging Kit (Invitrogen C10340). For immunofluorescent staining, cells were incubated in primary antibodies overnight in IF buffer: anti-KRT20 (1:200, Cell Signaling Technologies, #13063). They were then washed 3 times with PBS 0.1% Tween. The wells were then incubated with secondary antibodies (1:1000) in the IF buffer for 3 hours. The solution was removed and DAPI in PBS was added for 5 minutes and washed twice with PBS 0.1% Tween. The chambers were then removed and cover slips were mounted using Prolong Gold antifade medium (Invitrogen P36930).

Human normal colon and tumor organoid isolation and culture

Isolation of human colonic crypts and adenomas; culture and maintenance of organoid cultures were performed as previously described[32]. Normal and adenoma tissues were collected from colonic resections according to protocols approved by the Weill Cornell Medicine Institutional Review Board. Briefly, human colonic mucosa samples were obtained by trimming surgically resected specimens. The underlying muscle layer was removed using fine scissors under a stereomicroscope leaving the mucosa, which was cut into 5-mm pieces on a Petri dish, placed into a 15-ml centrifuge tube containing 10 ml of cold DPBS and washed 3 times. 10-ml of cold DPBS supplemented with 2.5 mM EDTA was added to the tube and incubated for 1hr room temp with gentle shaking. Isolated crypts were mixed with Matrigel (Corning, 354230), dispensed in the center of each well of a 6 well plate using a 200-µl pipette and placed at 37 °C for 10 min to solidify the Matrigel.

Normal colon organoids were also procured from Jason Spence's laboratory at the University of Michigan as previously described[33,34](specifically hCO lines 87 and 89). Normal human colon organoids (hCOs) were passaged 1:3 every 7 days by mechanical dissociation (pipetting) and grown in 12 well low

attachment plates in 30µl Matrigel droplets. Normal hCOs were cultured in normal human colon media (**Supplementary Data 3**) comprised of Advanced DMEM/F12, Pen/Strep, 4mM glutamax, 1% HEPES, primocin (100µg/ml), 50% L-WRN (Wnt3a, R-spondin, Noggin) conditioned media, N2, B27 without vitamin A, N-acetylcysteine (1mM), human recombinant EGF (50ng/ml), Y-27632 (10µM), A-83-01 (500nM), SB202190 (10µM). The L-WRN conditioned medium was generated by using L-WRN cells. Conditioned media was collected for 4 days pooled, sterile-filtered and frozen into aliquots until usage.

Human colorectal cancer organoids (hCRCO) were procured through the Institute for Precision Medicine at Weill Cornell Medicine[35]. The hCRCO were split 1:3 every 7 days by digesting in TrypLE Select (Thermofisher) supplemented with 10µM Y27632 (Tocris Bioscience), and were maintained in human colorectal cancer organoid media and propagated in Growth-factor-reduced Matrigel. Human colorectal cancer organoid is (**Supplementary Data 3**) comprised of Advanced DMEM/F12, 1%Pen/Strep, 1% glutamax, 1% HEPES, R-spondin1 conditioned media (5%) N-acetylcysteine (1.25mM), human recombinant EGF (50ng/ml), human recombinant FGF-10 (20ng/ml), FGF-2 (1 ng/ml), Y-27632 (10µM), A-83-01 (500nM), SB202190 (10µM), Nicotinamide (10mM), PGE2 (1µM), NRG (10 ng/ml), Human Gastrin1 (10nM) and propagated in GFR Matrigel.

Normal and tumor human organoid co-cultures with ECs

R-VEC or control CTRL-EC (at a final concentration of 5 million cells/ml) were mixed with normal human colon (hCO) or patient-derived tumor organoids (hCRCO), spun down and resuspended in Matrigel (Corning, 354230) or L.E.C mixture as described above. The cells were then dispersed in 30-70 µl Matrigel or L.E.C droplets in 8-well chamber slides (Lab-Tek II, 154534) or Nunc IVF 4-well dish (Thermo Scientific, cat# 144444) cultured in the respective organoid media with the addition of FGF-2 (10ng/ml) (Peprotech, 1000-18B) and heparin (100µg/ml) (Sigma H3149-100KU). Media was changed every other day. A 4.5 hour pulse of EdU was used for all tumor organoid co-culture experiments (Click-iT EdU kit, Invitrogen C10340). The co-cultures were maintained in 37^{o}C incubator with 20% oxygen. Triple negative breast cancer organoids were also procured from the Institute of Precision Medicine at Weill Cornell Medicine; media for maintenance and co-culture was the same as for human colorectal cancer organoids described above (minus the presence of Gastrin). Normal and tumor colon organoids were stained similarly to mouse small intestinal organoid co-cultures. Antibodies against human EpCAM (Biolegend) and VEcad (R&D) were incubated overnight, followed by secondary antibody staining.

For single-cell sequencing, co-cultures were maintained for 7 days. To collect cells in co-culture for single-cell sequencing, the medium was removed from the culture and the organoid- endothelial cell droplets were incubated in 2mg/ml of Dispase (Roche) for 20 min at 37^{o}C with shaking. The cells were then spun down and incubated for an additional 15 min at 37 ^{o}C in accutase. At this point, the endothelial cells were mostly released from the co-cultures and collected by filtering through a 40µm mesh. The rest of the

undigested cells (mainly organoid clusters) were further dissociated into single cells by incubating with TryplE for an additional 45 mins at 37^{o}C until the cells were completely separated as single cells. This two-step digestion allowed for increased viability and efficient dissociation of both endothelial cells and organoids. Both the first and the second fraction were further processed for single cell analysis. Single cells were collected and filtered through a 35µm nylon mesh and processed for single-cell sequencing.

For quantitative RT-PCR experiments, co-cultures were maintained for 7 days in Matrigel. To collect cells and dissociate organoids in co-cultures, we incubated the Matrigel droplets with TrypLE-Express enzyme (Thermo Fisher Scientific, 3ml/ 50µl Matrigel droplet) for 45 mins at 37^{o}C with vigorous shaking. The dissociated cells were then washed twice, once with organoid culture medium and once with MACs buffer. Dissociated cells were resuspended in 100µL of MACS buffer and anti-human CD31 (Biolegend, 10µg/ml) was used to stain for endothelial cells for 30mins on ice. The cell suspension was washed with MACS buffer and resuspended in MACS buffer with DAPI (1µg/ml). Subsequently, cells were sorted to purify the DAPI^{-}CD31^{-} population. Accurus PicoPure RNA isolation kit (ThermoFisher) was used to isolate RNA from the collected cells.

Quantifying interacting vessels with patient derived normal and tumor colon organoids documented in serial confocal videos

Human colorectal cancer organoids (hCRCO) and normal colon (hCO) organoids were stained with CellTracker (Invitrogen, C34565) per instruction manual of the manufacturer. Tumor and normal colon organoids were embedded inside Matrigel or L.E.C with either CTRL-ECs or R-VECs at 5million cells/ml. A mixture of gel and cells was pipetted onto glass-bottom dish and polymerized inside 37^{o}C incubator for 15mins. The culture was then fed with organoid medium supplemented with 10ng/ml bFGF (Peprotech), and 100µg/ml Heparin (Sigma H3149-100KU). To enable long-term imaging, 6-hydroxy-2,5,7,8-tetramethylchroman-2-Carboxylic Acid (Sigma), as an antioxidant, was also added into the medium at 100µM. Immediately, the culture was mounted onto a temperature- and gas-controlled chamber. Time lapse videos were acquired with a Zeiss Cell Observer confocal spinning disk microscope (Zeiss) equipped with a Photometrics Evolve 512 EMCCD camera at an interval of 40mins over 3-4 days. Media was refreshed every two days.

To quantify the vessels interacting with normal and tumor colon organoids, Z-projection images of time-lapse videos from several time points were obtained using ImageJ. Custom MATLAB codes were written to quantify the interacting vessel areas with all individual organoids. The custom MATLAB codes are provided at the end of the Methods. Briefly, the code was used to manually trace the perimeter of all vessels where ECs were wrapping and tapping the organoids. The area of the manually traced interacting vessels was quantified and reported.

RNA Library Preparation and Sequence Data Analysis

RNA was isolated and purified using *Qiagen's Rneasy Mini Kit or* Accurus PicoPure RNA isolation kit (ThermoFisher). RNA quality was verified using an Agilent Technologies 2100 Bioanalyzer. RNA library preps were prepared and multiplexed using Illumina TruSeq RNA Library Preparation Kit v2 (non-stranded and poly-A selection) and 10 nM of cDNA was used as input for high-throughput sequencing via Illumina's HiSeq 2500 or HiSeq 4000 producing 51 bp paired-end reads. Sequencing reads were de-multiplexed (bcl2fastq) and mapped with STAR v2.6.0c[36] with default parameters to the appropriate NCBI reference genome (GRCh38.p12 for human samples and GRCm38.p6 for mouse samples). Fragments per gene were counted with featureCounts v1.6.2[37] with respect to Gencode comprehensive gene annotations (release 28 for human samples and M17 for mouse samples).

Transcriptome Data Analysis

Differential gene expression analysis was performed using DESeq2 v1.18.1[38], and only FDR adjusted P-values <0.05 were considered statistically significant. Prior to differential gene expression analysis, lowly expressed genes were filtered out by only keeping genes that have more than 1 counts-per-million (CPM) in the condition with the least number of replicates. Base-2 log-transformed CPM values were used for heatmap plots, which were centered and scaled by row. Prior to visualization, tissue-specific effects were removed using the removeBatchEffect function from limma v3.34.9[39]. Gene ontology analysis was performed using DAVID Bioinformatics Resource Tools v 6.8[40].

ChIP and antibodies

To identify genome-wide localization of ETV2, K4me3, K27me3 and K27ac modification in R-VEC or CTRL-EC, ChIP assays were performed with approximately $1x10^7$ cells per experiment as previously described[41]. Cells introduced with triple flagged ETV2 lentivirus (as described above) were used for the ETV2 ChIP. Briefly, cells were crosslinked in 1% paraformaldehyde (PFA) for 10 min at 37°C, then quenched by 0.125M glycine. Chromatin was sheared using a Bioruptor (Diagenode) to create fragments of 200-400 bp, immunoprecipitated by 2–5 μg of antibody or mouse IgG bound to 75 μl Dynabeads M-280 (Invitrogen) and incubated overnight at 4°C. Magnetic beads were washed and chromatin was eluted. The ChIP DNA was reverse-crosslinked and column-purified. All ChIP antibodies are identified in the attached table below.

ChIP-seq library construction and sequencing

ChIP-seq libraries were prepared with the Illumina TruSeq ChIP Library Preparation Kit for DNA from ETV2 ChIP, and K4me3, K27me3 and K27ac modification ChIP. ChIP-seq libraries were sequenced with Illumina HiSeq 4000 system.

ChIP-seq data processing and analysis

ChIP-seq reads were aligned to the reference human genome (hg19, Genome Reference Consortium GRCh37) using the BWA alignment software (version 0.5.9)[42]. Unique reads mapped to a single best-matching location with no more than 4% of the read length of mismatches were kept for peak identification and profile generation. Sequence data were visualized with IGV by normalizing to 1 million reads[43] . The software MACS2[44] was applied to the ChIP-seq data with sequencing data from input DNA as control to identify genomic enrichment (peak) of ETV2. SICER (version 1.1)[45] algorithm was applied to the ChIP-seq data with sequencing data from input DNA as a control to identify genomic regions with significant enrichment differences in different cell types. The resulting peaks were filtered by *p*-value<0.05 for ETV2 and FDR<0.01 for histone modifications. We computed the read counts in individual promoters by HOMER[46]. Each identified peak was annotated to promoters (±2 kb from transcription start site), gene body, or intergenic region by HOMER.

10x Chromium single cell transcriptomics and analysis

The following two experiments were performed for single-cell library preparation to establish an adaptation of R-VECs upon co-culture with normal or malignant organoids:

Experiment 1: R-VECs were co-cultured alone or together with hCOs for 7 days in normal human colon organoid media supplemented with 10ng/ml FGF2 (Promocell) and 100µg/ml Heparin. hCOs were also cultured alone in normal human colon organoid media supplemented with 10ng/ml FGF and 100µg/ml Heparin for 7 days. After 7 days, all three conditions (R-VEC alone, R-VEC + hCOs or hCO alone) were dissociated with dispase and TryplE (Thermofisher) as described above and submitted for 10x Chromium single-cell analysis. All three samples were processed and run at the same time.

Experiment 2: R-VECs were co-cultured alone or together with Human Colorectal Cancer Organoids (hCRCO) for 7 days in colorectal cancer organoid media supplemented with 10ng/ml FGF2 and 100µg/ml Heparin. The hCRCOs were also cultured alone in colorectal cancer organoid media with 10ng/ml FGF and 100µg/ml Heparin for 7 days. After 7 days, all three conditions (R-VEC alone, R-VEC + hCRCO, or hCRCO alone) were dissociated with collagenase, dispase and TryplE (as described above) and submitted for 10x Chromium single-cell analysis. All three samples were processed and run at the same time.

The single cell suspension was loaded onto a well on a 10x Chromium Single Cell instrument (10x Genomics). Barcoding and cDNA synthesis were performed according to the manufacturer's instructions. Briefly, the 10x™ GemCode™ Technology partitions thousands of cells into nanoliter-scale Gel Bead-In-EMulsions (GEMs), where all the cDNA generated from an individual cell share a common 10x Barcode. In order to identify the PCR duplicates, Unique Molecular Identifier (UMI) was also added. The GEMs were incubated with enzymes to produce full length cDNA, which was then amplified by PCR to generate enough quantity for library construction. Qualitative analysis was performed using the Agilent Bioanalyzer High

Sensitivity assay. The cDNA libraries were constructed using the 10x ChromiumTM Single cell 3' Library Kit according to the manufacturer's original protocol. Briefly, after the cDNA amplification, enzymatic fragmentation and size selection were performed using SPRI select reagent (Beckman Coulter, Cat# B23317) to optimize the cDNA size. P5, P7, a sample index and read 2 (R2) primer sequence were added by end repair, A-tailing, adaptor ligation and sample-index PCR. The final single cell 3' library contains a standard Illumina paired-end constructs (P5 and P7), Read 1 (R1) primer sequence, 16 bp 10x barcode, 10 bp randomer, 98 bp cDNA fragments, R2 primer sequence and 8 bp sample index. For post library construction QC, 1ul of the ssample was diluted 1:10 and ran on the Agilent Bioanalyzer High Sensitivity chip for qualitative analysis. For quantification, Illumina Library Quantification Kit (KAPA Biosystems, Cat# KK4824) was used.

Libraries were sequenced on Illumina NextSeq500 with 150 cycle kit using the following read length: 26bp Read1 for cell barcode and UMI, 8bp I7 index for sample index and 132bp Read2 for transcript. Cell Ranger 2.2.0 (http://10xgenomics.com) was used to process Chromium single cell 3' RNA-seq output. First, "cellranger mkfastq" demultiplexed the sequencing samples based on the 8bp sample index read to generate fastq files for the Read1 and Read2, followed by extraction of 16bp cell barcode and 10bp UMI. Second, "cellranger count" aligned the Read2 to the human reference genome (GRCh38) using STAR[36]. Then, aligned reads were used to generate data matrix only when they have valid barcodes and UMI, map to exons (Ensembl GRCh38) without PCR duplicates. Valid cell barcodes were defined based on UMI distribution.

All single-cell analyses were performed using the Seurat package in R (version 2.3.4)[47]. Once the gene-cell data matrix was generated, poor quality cells were excluded, including cells with more than 6,000 unique expressed genes (as they are potentially cell doublets). Only genes expressed in 3 or more cells in a sample were used for further analysis. Cells were also discarded if their mitochondrial gene percentages were over 10% or if they expressed less than 600 unique genes, resulting in 20,778 genes across 24,478 cells and median UMI count for each cell across the entire dataset being 7,845 and the median number of unique genes per cell being 2,397. Further information on each sample passing quality filters is available in Extended Table 1 below. Following best practices in the package suggestions UMI counts were log-normalized and after the most highly variable genes selected the data matrices were scaled using a linear model with variation arising from UMI counts and mitochondrial gene expression mitigated for. The principal component analysis was subsequently performed on this matrix and after reviewing principal component heatmaps and jackstraw plots Uniform Manifold Approximation and Projection (UMAP) visualization were performed on the top 29 components and clustering resolution was set at 1.0 for visualizations. Differential gene expression for gene marker discovery across the clusters were performed using the Wilcoxon rank-sum test as used in the Seurat package.

Epithelial cells were identified by epithelial cell markers EpCAM, CDH1, KRT19 and eECs were identified by EC markers VEcadherin (CDH5), PECAM1 (CD31) and VEGFR2 (KDR). Subsequent to this, epithelial cells were filtered out from the next analysis to identify heterogeneity amongst the EC populations of the co-cultured normal and tumor cell populations. The epithelial cell fraction was also analyzed on its own in the tumor and co-cultured samples. In both these analyses best practices were again followed for cluster discovery using the top 20 components and cluster resolution 0.6 in the matched tumor and normal sample sets and differential gene expression for gene marker discovery across the clusters were performed using the Wilcoxon rank-sum test as used in the Seurat package.

Statistical analysis

Data were assessed and analyzed using appropriate statistical methods. The normality of data was assessed using the Kolmogorov-Smirnov test. Sample sizes and statistics for each experiment are provided in **Supplementary Data 2**. GraphPad Prism 7 was used for all statistical analysis, unless otherwise indicated. No statistics were used to determine sample size.

Reporting summary

Information on research design is available in the Nature Research Reporting Summary linked to this paper.

Data availability

Source data for Figs. 1-4 and Extended Data Figs.1,2,3,5,6,7,8 are available as .xsl tables with the paper. Source data for ChIP-sequencing can be found in Supplementary Table 1 and source data for single cells RNA-sequencing can be found in Supplementary Table 2. The RNA-sequencing data can be viewed on GEO under the record GSE131039. The ChIP-sequencing data can be viewed on GEO under the record GSE147746. The single-cell RNA-sequencing data can be viewed on GEO under the record GSE148996.

Code availability

All code utilized in this paper is available from the authors upon request.

Acknowledgements:

SR: Ansary Stem Cell Institute, grants from the National Institute of health (NIH), R35 HL150809, R01s DK095039, HL119872, HL128158, HL115128, HL139056, RC2 DK114777, U01AI138329, the Empire State Stem Cell Board and New York State Department of Health grants (NYSTEM) (C026878, C028117, C029156, C030160), Daedalus Fund for Innovation from Weill Cornell Medicine, the Starr Foundation stem cell core project and initiatives TRI-SCI #2013-032, #2014-023, #2016-013, #2019-029. RS: NYSTEM contract C32596GG. PDC is supported by NIH Research (NIHR-RP-2014-04-046). P.D.C., A.P., A.M.T.,

F.S.: OAK Foundation (W1095/OCAY-14-191), H2020 grant INTENS 668294, and NIHR Biomedical Research Centre at Great Ormond Street Hospital for Children NHS Foundation Trust. AMT.: BBSRC ICASE studentship 167881. YLiu and JMGS: New York Stem Cell Foundation, Druckenmiller Fellowship. BK: T32 Fellowship. OE: NIH UL1TR002384, R01CA194547, LLS SCOR 180078-02, 7021-20. JRS: HL119215. QJZ: DK106253, UC4116280. We thank the Visual Function Core at Weill Cornell Medicine live imaging resources, Claude Wasserstein, Marcia Mishaan, Matthew Bell, Cynthia Cheung and Wei Gu for support with organoid cultures and Asllan Gjinovci for the surgical help with mouse small bowel isolation.

Competing interests: SR is the founder and a non-paid consultant to Angiocrine Bioscience, San Diego, CA, USA. OE is supported by Janssen and Eli Lilly research grants, and is scientific advisor and equity holder in Freenome, Owkin, Volastra Therapeutics and One Three Biotech.

Author contribution: BP and SR conceived of the study and wrote the manuscript. BP, DTN, RS, KS, RES, SYR and SR discussed and analyzed data. RS provided microscopy expertise. BP, DTN, GL, RS, YLiu, FG, YLin, JMGS, MY, SYR, SR performed experiments and analyzed data. AFP, AMT, FS and PDC carried out and analyzed experiments on the decellularized intestines. YLiu, DR, PZ, TZ, BK, OE, JX analyzed ChIP, RNA and single cell sequencing. MW, TH, SL, LD, JS, QJZ assisted with organoid cultures. All the authors read and provided feedback on the figures and manuscript.

References:

1 Augustin, H. G. & Koh, G. Y. Organotypic vasculature: From descriptive heterogeneity to functional pathophysiology. *Science* **357**, doi:10.1126/science.aal2379 (2017).

2 Rafii, S., Butler, J. M. & Ding, B. S. Angiocrine functions of organ-specific endothelial cells. *Nature* **529**, 316-325, doi:10.1038/nature17040 (2016).

3 Lee, D. *et al.* ER71 acts downstream of BMP, Notch, and Wnt signaling in blood and vessel progenitor specification. *Cell Stem Cell* **2**, 497-507, doi:10.1016/j.stem.2008.03.008 (2008).

4 Barry, D. M. *et al.* Rasip1-Mediated Rho GTPase Signaling Regulates Blood Vessel Tubulogenesis via Nonmuscle Myosin II. *Circ Res* **119**, 810-826, doi:10.1161/CIRCRESAHA.116.309094 (2016).

5 Strilic, B. *et al.* The molecular basis of vascular lumen formation in the developing mouse aorta. *Dev Cell* **17**, 505-515, doi:10.1016/j.devcel.2009.08.011 (2009).

6 Carmeliet, P. & Jain, R. K. Molecular mechanisms and clinical applications of angiogenesis. *Nature* **473**, 298-307, doi:10.1038/nature10144 (2011).

7 Cao, Z. *et al.* Molecular Checkpoint Decisions Made by Subverted Vascular Niche Transform Indolent Tumor Cells into Chemoresistant Cancer Stem Cells. *Cancer Cell* **31**, 110-126, doi:10.1016/j.ccell.2016.11.010 (2017).

8 Nolan, D. J. *et al.* Molecular signatures of tissue-specific microvascular endothelial cell heterogeneity in organ maintenance and regeneration. *Dev Cell* **26**, 204-219, doi:10.1016/j.devcel.2013.06.017 (2013).

9 Pellegata, A. F., Tedeschi, A. M. & De Coppi, P. Whole Organ Tissue Vascularization: Engineering the Tree to Develop the Fruits. *Front Bioeng Biotechnol* **6**, 56, doi:10.3389/fbioe.2018.00056 (2018).

10 Giobbe, G. G. *et al.* Extracellular matrix hydrogel derived from decellularized tissues enables endodermal organoid culture. *Nature Communications* **10**, 1-14, doi:doi:10.1038/s41467-019-13605-4 (2019).

11 Ronaldson-Bouchard, K. & Vunjak-Novakovic, G. Organs-on-a-Chip: A Fast Track for Engineered Human Tissues in Drug Development. *Cell Stem Cell* **22**, 310-324, doi:10.1016/j.stem.2018.02.011 (2018).

12 Bhatia, S. N. & Ingber, D. E. Microfluidic organs-on-chips. *Nat Biotechnol* **32**, 760-772, doi:10.1038/nbt.2989 (2014).

13 Lancaster, M. A. & Knoblich, J. A. Organogenesis in a dish: modeling development and disease using organoid technologies. *Science* **345**, 1247125, doi:10.1126/science.1247125 (2014).

14 Tuveson, D. & Clevers, H. Cancer modeling meets human organoid technology. *Science* **364**, 952-955, doi:10.1126/science.aaw6985 (2019).

15 Koyano-Nakagawa, N. & Garry, D. J. Etv2 as an essential regulator of mesodermal lineage development. *Cardiovasc Res* **113**, 1294-1306, doi:10.1093/cvr/cvx133 (2017).

16 Ginsberg, M. *et al.* Efficient Direct Reprogramming of Mature Amniotic Cells into Endothelial Cells by ETS Factors and TGFbeta Suppression. *Cell* **151**, 559-575, doi:S0092-8674(12)01178-6 [pii]10.1016/j.cell.2012.09.032 (2012).

17 Nguyen, D. H. *et al.* Biomimetic model to reconstitute angiogenic sprouting morphogenesis in vitro. *Proc Natl Acad Sci U S A* **110**, 6712-6717, doi:10.1073/pnas.1221526110 (2013).

18 Eberhard, D., Kragl, M. & Lammert, E. 'Giving and taking': endothelial and beta-cells in the islets of Langerhans. *Trends Endocrinol Metab* **21**, 457-463, doi:10.1016/j.tem.2010.03.003 (2010).

19 Sato, T. *et al.* Long-term expansion of epithelial organoids from human colon, adenoma, adenocarcinoma, and Barrett's epithelium. *Gastroenterology* **141**, 1762-1772, doi:10.1053/j.gastro.2011.07.050 (2011).

20 Miyoshi, H. & Stappenbeck, T. S. In vitro expansion and genetic modification of gastrointestinal stem cells in spheroid culture. *Nature Protocols* **8**, 2471-2482, doi:doi:10.1038/nprot.2013.153 (2013).

21 Stan, R. V. *et al.* The diaphragms of fenestrated endothelia – gatekeepers of vascular permeability and blood composition. *Dev Cell* **23**, 1203-1218, doi:10.1016/j.devcel.2012.11.003 (2012).

22 Lyden, D. *et al.* Id1 and Id3 are required for neurogenesis, angiogenesis and vascularization of tumour xenografts. *Nature* **401**, 670-677, doi:10.1038/44334 (1999).

23 Li, S. *et al.* in *J Cancer* Vol. 8 1355-1361 (2017).
24 Si, M. & Lang, J. in *J Hematol Oncol* Vol. 11 (2018).

Extended References:

25 Baudin, B., Bruneel, A., Bosselut, N. & Vaubourdolle, M. A protocol for isolation and culture of human umbilical vein endothelial cells. *Nature Protocols* **2**, 481, doi:doi:10.1038/nprot.2007.54 (2007).
26 Seandel, M. *et al.* Generation of a functional and durable vascular niche by the adenoviral E4ORF1 gene. *Proc Natl Acad Sci U S A* **105**, 19288-19293, doi:10.1073/pnas.0805980105 (2008).
27 Ginsberg, M., Schachterle, W., Shido, K. & Rafii, S. Direct conversion of human amniotic cells into endothelial cells without transitioning through a pluripotent state. *Nat Protoc* **10**, 1975-1985, doi:10.1038/nprot.2015.126 (2015).
28 Schachterle, W. *et al.* Sox17 drives functional engraftment of endothelium converted from non-vascular cells. *Nat Commun* **8**, 13963, doi:10.1038/ncomms13963 (2017).
29 Wareing, S., Eliades, A., Lacaud, G. & Kouskoff, V. ETV2 expression marks blood and endothelium precursors, including hemogenic endothelium, at the onset of blood development. *Dev Dyn* **241**, 1454-1464, doi:10.1002/dvdy.23825 (2012).
30 Zudaire, E., Gambardella, L., Kurcz, C. & Vermeren, S. A computational tool for quantitative analysis of vascular networks. *PLoS One* **6**, e27385, doi:10.1371/journal.pone.0027385 (2011).
31 Sato, T. *et al.* Single Lgr5 stem cells build crypt-villus structures in vitro without a mesenchymal niche. *Nature* **459**, 262-265, doi:10.1038/nature07935 (2009).
32 Sugimoto, S. & Sato, T. Establishment of 3D Intestinal Organoid Cultures from Intestinal Stem Cells. *Methods Mol Biol* **1612**, 97-105, doi:10.1007/978-1-4939-7021-6_7 (2017).
33 Dame, M. K. *et al.* Identification, isolation and characterization of human LGR5-positive colon adenoma cells. *Development* **145**, doi:10.1242/dev.153049 (2018).
34 Tsai, Y. H. *et al.* A Method for Cryogenic Preservation of Human Biopsy Specimens and Subsequent Organoid Culture. *Cell Mol Gastroenterol Hepatol* **6**, 218-222.e217, doi:10.1016/j.jcmgh.2018.04.008 (2018).
35 Puca, L. *et al.* Patient derived organoids to model rare prostate cancer phenotypes. *Nature Communications* **9**, 1-10, doi:doi:10.1038/s41467-018-04495-z (2018).
36 Dobin, A. *et al.* STAR: ultrafast universal RNA-seq aligner. *Bioinformatics* **29**, 15-21, doi:10.1093/bioinformatics/bts635 (2013).
37 Liao, Y., Smyth, G. K. & Shi, W. featureCounts: an efficient general purpose program for assigning sequence reads to genomic features. *Bioinformatics* **30**, 923-930, doi:10.1093/bioinformatics/btt656 (2014).
38 Love, M. I., Huber, W. & Anders, S. Moderated estimation of fold change and dispersion for RNA-seq data with DESeq2. *Genome Biol* **15**, 550, doi:10.1186/s13059-014-0550-8 (2014).
39 Ritchie, M. E. *et al.* limma powers differential expression analyses for RNA-sequencing and microarray studies. *Nucleic Acids Res* **43**, e47, doi:10.1093/nar/gkv007 (2015).
40 Huang da, W., Sherman, B. T. & Lempicki, R. A. Systematic and integrative analysis of large gene lists using DAVID bioinformatics resources. *Nat Protoc* **4**, 44-57, doi:10.1038/nprot.2008.211 (2009).
41 Liu, Y. *et al.* Epigenetic profiles signify cell fate plasticity in unipotent spermatogonial stem and progenitor cells. *Nat Commun* **7**, 11275, doi:10.1038/ncomms11275 (2016).
42 Li, H. & Durbin, R. Fast and accurate short read alignment with Burrows-Wheeler transform. *Bioinformatics* **25**, 1754-1760, doi:10.1093/bioinformatics/btp324 (2009).
43 Thorvaldsdottir, H., Robinson, J. T. & Mesirov, J. P. Integrative Genomics Viewer (IGV): high-performance genomics data visualization and exploration. *Brief Bioinform* **14**, 178-192, doi:10.1093/bib/bbs017 (2013).
44 Zhang, Y. *et al.* Model-based analysis of ChIP-Seq (MACS). *Genome Biol* **9**, R137, doi:10.1186/gb-2008-9-9-r137 (2008).

45 Zang, C. *et al.* A clustering approach for identification of enriched domains from histone modification ChIP-Seq data. *Bioinformatics* **25**, 1952-1958, doi:10.1093/bioinformatics/btp340 (2009).
46 Heinz, S. *et al.* Simple combinations of lineage-determining transcription factors prime cis-regulatory elements required for macrophage and B cell identities. *Mol Cell* **38**, 576-589, doi:10.1016/j.molcel.2010.05.004 (2010).
47 Butler, A., Hoffman, P., Smibert, P., Papalexi, E. & Satija, R. Integrating single-cell transcriptomic data across different conditions, technologies, and species. *Nature Biotechnology* **36**, 411, doi:doi:10.1038/nbt.4096 (2018).

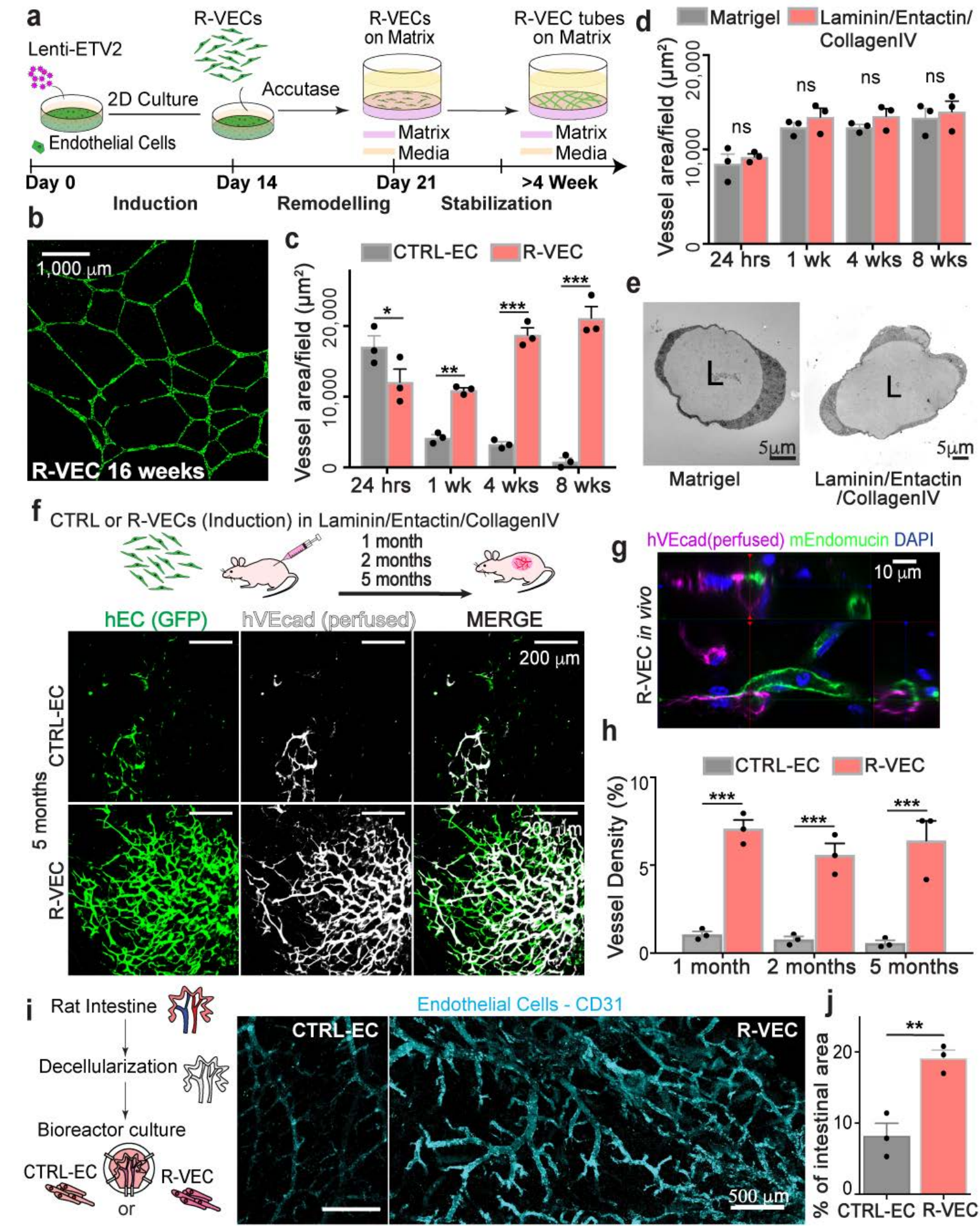
a
Lenti-ETV2
2D Culture
Endothelial Cells
R-VECs
Accutase
R-VECs on Matrix
Matrix
Media
R-VEC tubes on Matrix
Matrix
Media
Day 0
Day 14
Day 21
>4 Week
Induction
Remodelling
Stabilization
b
1,000 μm
R-VEC 16 weeks
c
CTRL-EC
R-VEC
Vessel area/field (μm²)
0
10,000
20,000
*
**
***
***
24 hrs
1 wk
4 wks
8 wks
d
Matrigel
Laminin/Entactin/ CollagenIV
Vessel area/field (μm²)
0
10,000
20,000
ns
ns
ns
ns
24 hrs
1 wk
4 wks
8 wks
e
L
5μm
Matrigel
L
5μm
Laminin/Entactin /CollagenIV
f
CTRL or R-VECs (Induction) in Laminin/Entactin/CollagenIV
1 month
2 months
5 months
hEC (GFP)
hVEcad (perfused)
MERGE
200 μm
CTRL-EC
5 months
R-VEC
200 μm
g
hVEcad(perfused) mEndomucin DAPI
10 μm
R-VEC in vivo
h
CTRL-EC
R-VEC
Vessel Density (%)
0
5
10
***
***
***
1 month
2 months
5 months
i
Rat Intestine
Decellularization
Bioreactor culture
CTRL-EC
R-VEC
or
Endothelial Cells - CD31
CTRL-EC
R-VEC
500 μm
j
% of intestinal area
0
10
20
**
CTRL-EC
R-VEC

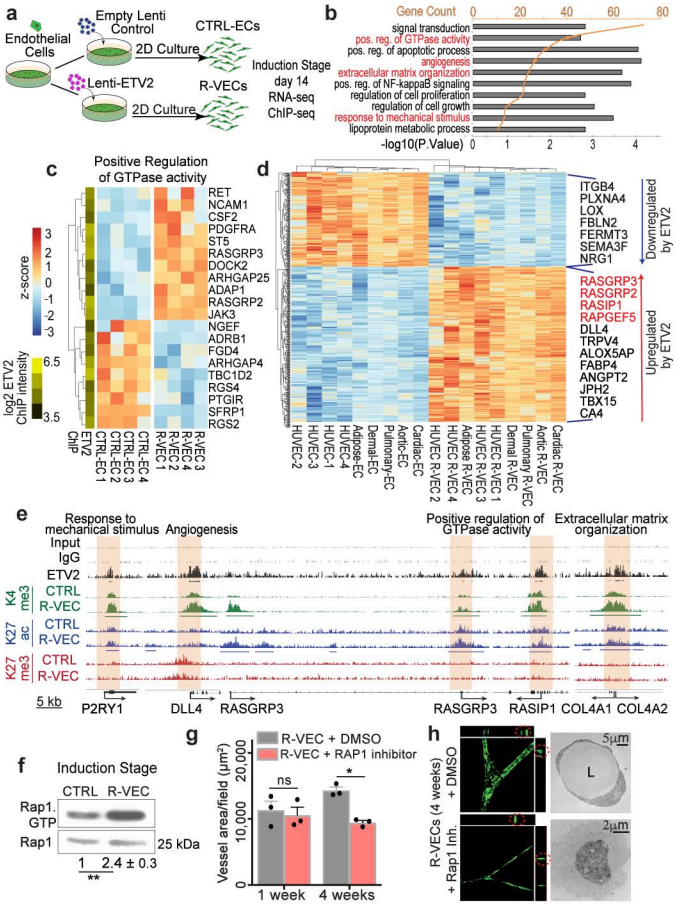
a
Endothelial Cells
Empty Lenti Control
2D Culture
CTRL-ECs
Lenti-ETV2
2D Culture
R-VECs
Induction Stage
day 14
RNA-seq
ChIP-seq
b
Gene Count
signal transduction
pos. reg. of GTPase activity
pos. reg. of apoptotic process
angiogenesis
extracellular matrix organization
pos. reg. of NF-kappaB signaling
regulation of cell proliferation
regulation of cell growth
response to mechanical stimulus
lipoprotein metabolic process
-log10(P.Value)
c
Positive Regulation of GTPase activity
z-score
log2 ETV2 ChIP intensity
RET
NCAM1
CSF2
PDGFRA
ST5
RASGRP3
DOCK2
ARHGAP25
ADAP1
RASGRP2
JAK3
NGEF
ADRB1
FGD4
ARHGAP4
TBC1D2
RGS4
PTGIR
SFRP1
RGS2
ETV2 ChIP
CTRL-EC 1
CTRL-EC 2
CTRL-EC 3
CTRL-EC 4
R-VEC 1
R-VEC 2
R-VEC 3
R-VEC 4
d
ITGB4
PLXNA4
LOX
FBLN2
FERMT3
SEMA3F
NRG1
Downregulated by ETV2
RASGRP3
RASGRP2
RASIP1
RAPGEF5
DLL4
TRPV4
ALOX5AP
FABP4
ANGPT2
JPH2
TBX15
CA4
Upregulated by ETV2
HUVEC-2
HUVEC-3
HUVEC-1
HUVEC-4
Adipose-EC
Dermal-EC
Pulmonary-EC
Aortic-EC
Cardiac-EC
HUVEC R-VEC 2
HUVEC R-VEC 4
Adipose R-VEC
HUVEC R-VEC 3
HUVEC R-VEC 1
Dermal R-VEC
Pulmonary R-VEC
Aortic R-VEC
Cardiac R-VEC
e
Response to mechanical stimulus
Angiogenesis
Positive regulation of GTPase activity
Extracellular matrix organization
Input
IgG
ETV2
K4 me3
CTRL
R-VEC
K27 ac
CTRL
R-VEC
K27 me3
CTRL
R-VEC
5 kb
P2RY1
DLL4
RASGRP3
RASGRP3
RASIP1
COL4A1
COL4A2
f
Induction Stage
CTRL
R-VEC
Rap1 GTP
Rap1
25 kDa
1
2.4 ± 0.3
**
g
R-VEC + DMSO
R-VEC + RAP1 inhibitor
Vessel area/field (μm²)
20,000
10,000
0
ns
*
1 week
4 weeks
h
R-VECs (4 weeks)
+ DMSO
+ Rap1 Inh.
5μm
L
2μm

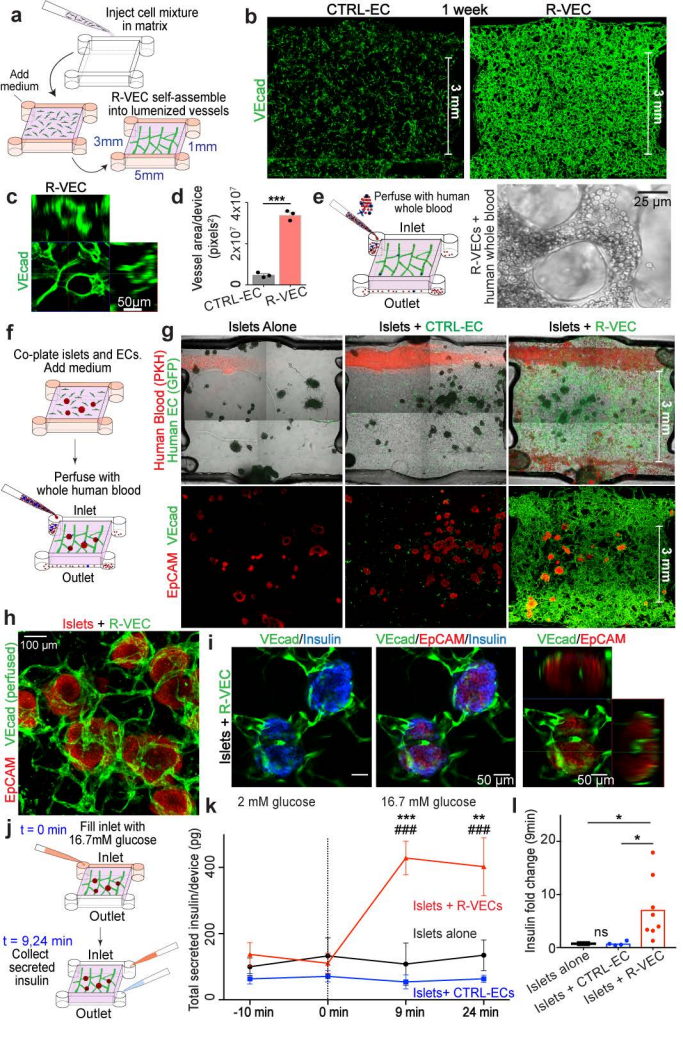
a
Inject cell mixture in matrix
Add medium
R-VEC self-assemble into lumenized vessels
3mm
1mm
5mm
b
CTRL-EC
1 week
R-VEC
VEcad
3 mm
3 mm
c
R-VEC
VEcad
50µm
d
Vessel area/device (pixels²)
2x10⁷
4x10⁷
0
***
CTRL-EC
R-VEC
e
Perfuse with human whole blood
Inlet
Outlet
R-VECs + human whole blood
25 µm
f
Co-plate islets and ECs. Add medium
Perfuse with whole human blood
Inlet
Outlet
g
Islets Alone
Islets + CTRL-EC
Islets + R-VEC
Human Blood (PKH)
Human EC (GFP)
EpCAM
VEcad
3 mm
3 mm
h
Islets + R-VEC
100 µm
VEcad (perfused)
EpCAM
i
VEcad/Insulin
VEcad/EpCAM/Insulin
VEcad/EpCAM
Islets + R-VEC
50 µm
50 µm
j
t = 0 min
Fill inlet with 16.7mM glucose
Inlet
Outlet
t = 9,24 min
Collect secreted insulin
Inlet
Outlet
k
2 mM glucose
16.7 mM glucose
*** ###
** ###
Total secreted insulin/device (pg)
0
200
400
Islets + R-VECs
Islets alone
Islets+ CTRL-ECs
-10 min
0 min
9 min
24 min
l
Insulin fold change (9min)
0
10
20
*
*
ns
Islets alone
Islets + CTRL-EC
Islets + R-VEC

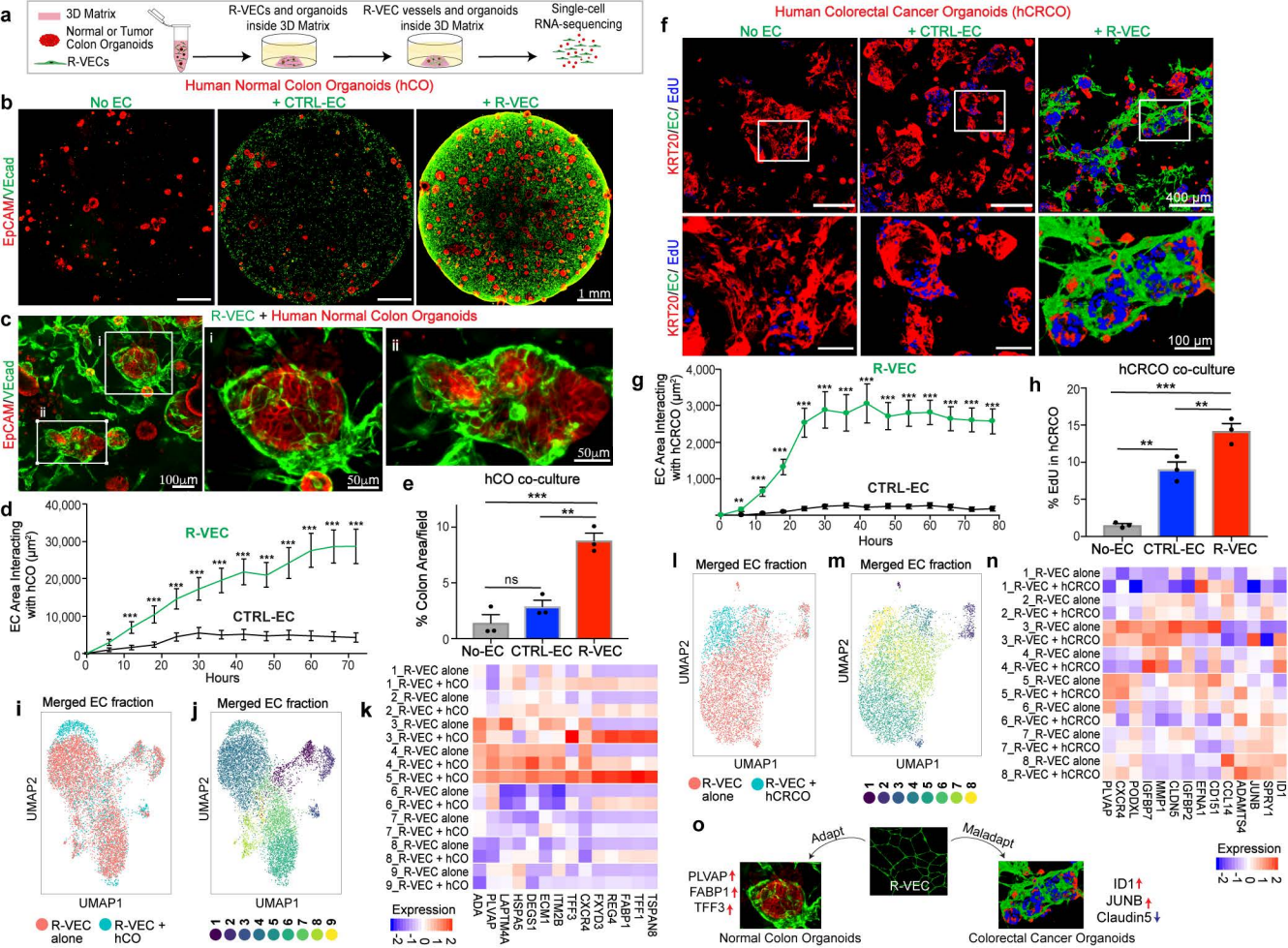
a
3D Matrix
Normal or Tumor Colon Organoids
R-VECs
R-VECs and organoids inside 3D Matrix
R-VEC vessels and organoids inside 3D Matrix
Single-cell RNA-sequencing
b
Human Normal Colon Organoids (hCO)
No EC
+ CTRL-EC
+ R-VEC
EpCAM/VEcad
1 mm
c
R-VEC + Human Normal Colon Organoids
EpCAM/VEcad
100μm
50μm
d
EC Area Interacting with hCO (μm²)
R-VEC
CTRL-EC
Hours
e
hCO co-culture
% Colon Area/field
ns
No-EC
CTRL-EC
R-VEC
f
Human Colorectal Cancer Organoids (hCRCO)
No EC
+ CTRL-EC
+ R-VEC
KRT20/EC/ EdU
400 μm
100 μm
g
R-VEC
EC Area Interacting with hCRCO (μm²)
CTRL-EC
Hours
h
hCRCO co-culture
% EdU in hCRCO
No-EC
CTRL-EC
R-VEC
i
Merged EC fraction
UMAP2
UMAP1
R-VEC alone
R-VEC + hCO
j
Merged EC fraction
UMAP2
UMAP1
k
1_R-VEC alone
1_R-VEC + hCO
2_R-VEC alone
2_R-VEC + hCO
3_R-VEC alone
3_R-VEC + hCO
4_R-VEC alone
4_R-VEC + hCO
5_R-VEC alone
5_R-VEC + hCO
6_R-VEC alone
6_R-VEC + hCO
7_R-VEC alone
7_R-VEC + hCO
8_R-VEC alone
8_R-VEC + hCO
9_R-VEC alone
9_R-VEC + hCO
ADA
PLVAP
LAPTM4A
HSPA5
DEGS1
EOM1
ITM2B
TFF3
CXCR4
FXYD3
REG4
FABP1
TFF1
TSPAN8
Expression
l
Merged EC fraction
UMAP2
UMAP1
R-VEC alone
R-VEC + hCRCO
m
Merged EC fraction
UMAP2
UMAP1
n
1_R-VEC alone
1_R-VEC + hCRCO
2_R-VEC alone
2_R-VEC + hCRCO
3_R-VEC alone
3_R-VEC + hCRCO
4_R-VEC alone
4_R-VEC + hCRCO
5_R-VEC alone
5_R-VEC + hCRCO
6_R-VEC alone
6_R-VEC + hCRCO
7_R-VEC alone
7_R-VEC + hCRCO
8_R-VEC alone
8_R-VEC + hCRCO
PLVAP
CXCR4
PODXL
IGFBP7
CLDN5
MMP1
IGFBP2
EFNA1
CD151
CCL14
ADAMTS4
JUNB
SPRY1
ID1
Expression
o
Adapt
Maladapt
R-VEC
PLVAP↑
FABP1↑
TFF3↑
Normal Colon Organoids
ID1↑
JUNB↑
Claudin5↓
Colorectal Cancer Organoids

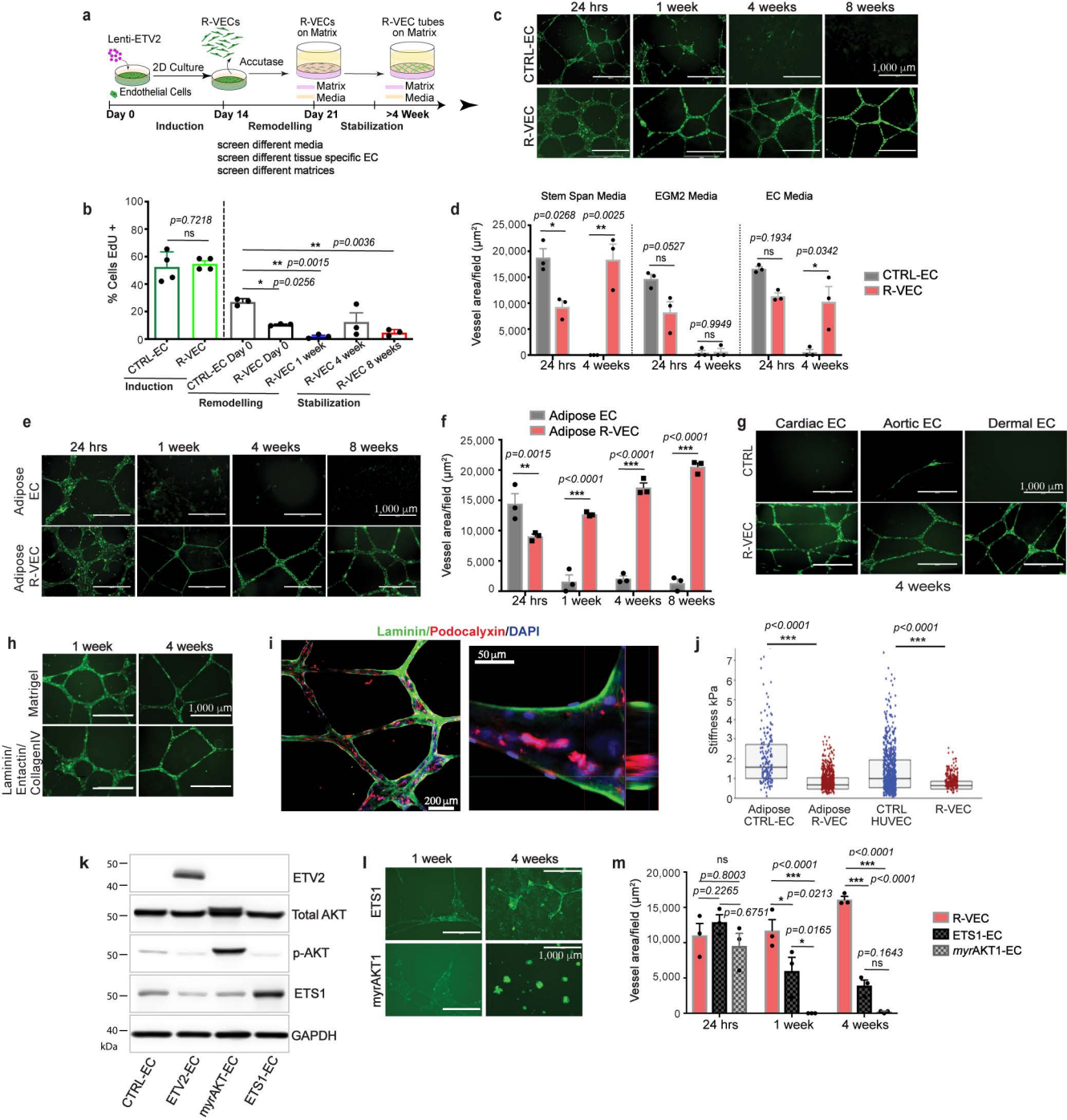
a
Lenti-ETV2
2D Culture
Endothelial Cells
R-VECs
Accutase
R-VECs on Matrix
Matrix
Media
R-VEC tubes on Matrix
Matrix
Media
Day 0
Induction
Day 14
Remodelling
Day 21
Stabilization
>4 Week
screen different media
screen different tissue specific EC
screen different matrices
c
24 hrs
1 week
4 weeks
8 weeks
CTRL-EC
R-VEC
1,000 μm
b
% Cells EdU +
p=0.7218
ns
p=0.0036
p=0.0015
p=0.0256
CTRL-EC
R-VEC
CTRL-EC Day 0
R-VEC Day 0
R-VEC 1 week
R-VEC 4 week
R-VEC 8 weeks
Induction
Remodelling
Stabilization
d
Stem Span Media
EGM2 Media
EC Media
Vessel area/field (μm²)
p=0.0268
p=0.0025
p=0.0527
ns
p=0.9949
ns
p=0.1934
ns
p=0.0342
CTRL-EC
R-VEC
24 hrs
4 weeks
e
24 hrs
1 week
4 weeks
8 weeks
Adipose EC
Adipose R-VEC
1,000 μm
f
Adipose EC
Adipose R-VEC
Vessel area/field (μm²)
p=0.0015
p<0.0001
p<0.0001
p<0.0001
24 hrs
1 week
4 weeks
8 weeks
g
Cardiac EC
Aortic EC
Dermal EC
CTRL
R-VEC
1,000 μm
4 weeks
h
1 week
4 weeks
Matrigel
Laminin/ Entactin/ CollagenIV
1,000 μm
i
Laminin/Podocalyxin/DAPI
50 μm
200 μm
j
p<0.0001
p<0.0001
Stiffness kPa
Adipose CTRL-EC
Adipose R-VEC
CTRL HUVEC
R-VEC
k
ETV2
Total AKT
p-AKT
ETS1
GAPDH
kDa
CTRL-EC
ETV2-EC
myrAKT1-EC
ETS1-EC
l
1 week
4 weeks
ETS1
myrAKT1
1,000 μm
m
Vessel area/field (μm²)
ns
p=0.8003
p=0.2265
p=0.6751
p<0.0001
p=0.0213
p=0.0165
p<0.0001
p<0.0001
p<0.0001
p=0.1643
ns
24 hrs
1 week
4 weeks
R-VEC
ETS1-EC
myrAKT1-EC

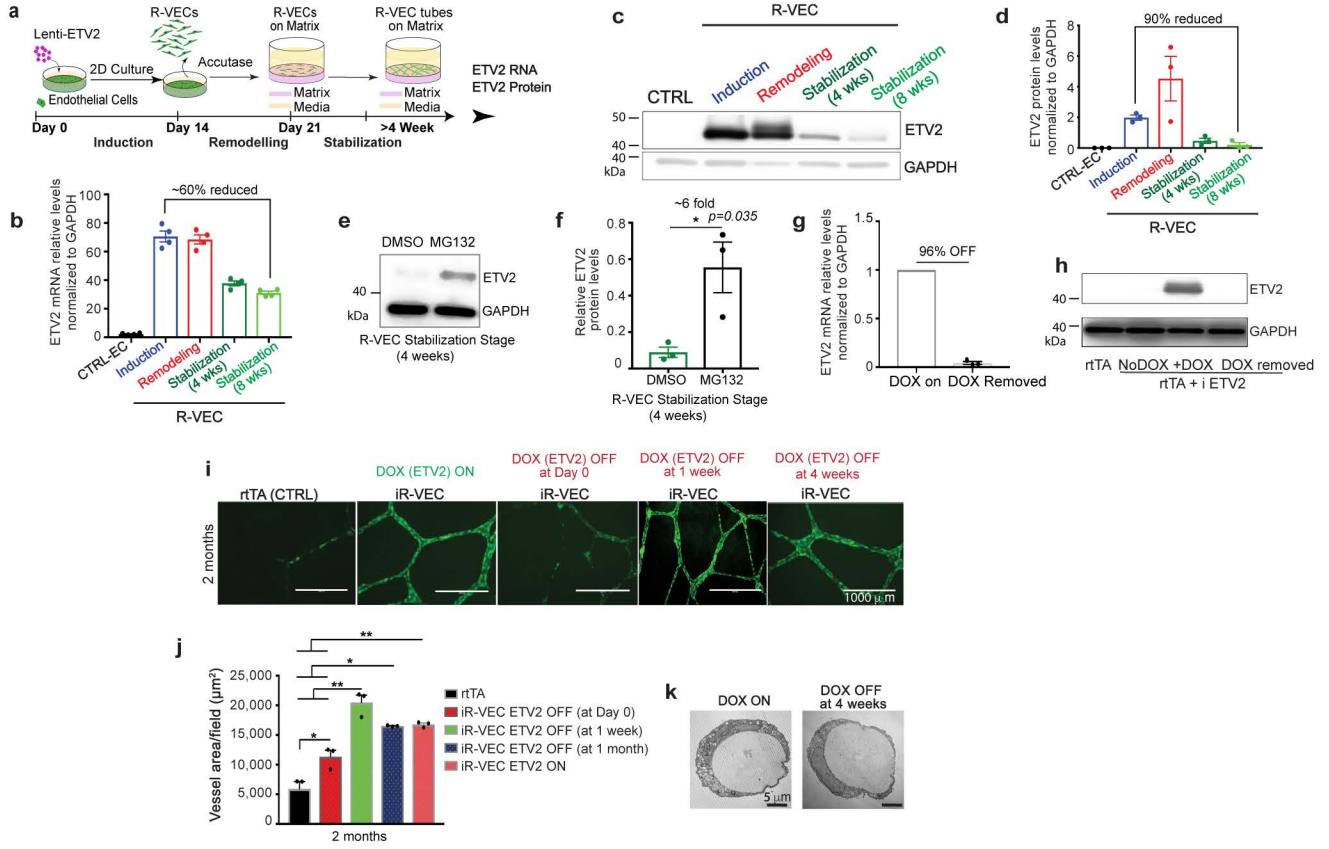
a
Lenti-ETV2
Endothelial Cells
2D Culture
R-VECs
Accutase
R-VECs on Matrix
Matrix
Media
R-VEC tubes on Matrix
Matrix
Media
ETV2 RNA
ETV2 Protein
Day 0
Induction
Day 14
Remodelling
Day 21
Stabilization
>4 Week
b
ETV2 mRNA relative levels normalized to GAPDH
~60% reduced
CTRL-EC
Induction
Remodeling
Stabilization (4 wks)
Stabilization (8 wks)
R-VEC
c
R-VEC
CTRL
Induction
Remodeling
Stabilization (4 wks)
Stabilization (8 wks)
ETV2
GAPDH
kDa
d
ETV2 protein levels normalized to GAPDH
90% reduced
R-VEC
e
DMSO MG132
ETV2
GAPDH
kDa
R-VEC Stabilization Stage (4 weeks)
f
Relative ETV2 protein levels
~6 fold
p=0.035
DMSO
MG132
R-VEC Stabilization Stage (4 weeks)
g
ETV2 mRNA relative levels normalized to GAPDH
96% OFF
DOX on
DOX Removed
h
ETV2
GAPDH
kDa
rtTA
NoDOX
+DOX
DOX removed
rtTA + i ETV2
i
rtTA (CTRL)
DOX (ETV2) ON
iR-VEC
DOX (ETV2) OFF at Day 0
DOX (ETV2) OFF at 1 week
DOX (ETV2) OFF at 4 weeks
2 months
1000 µm
j
Vessel area/field (µm²)
rtTA
iR-VEC ETV2 OFF (at Day 0)
iR-VEC ETV2 OFF (at 1 week)
iR-VEC ETV2 OFF (at 1 month)
iR-VEC ETV2 ON
2 months
k
DOX ON
DOX OFF at 4 weeks
5 µm

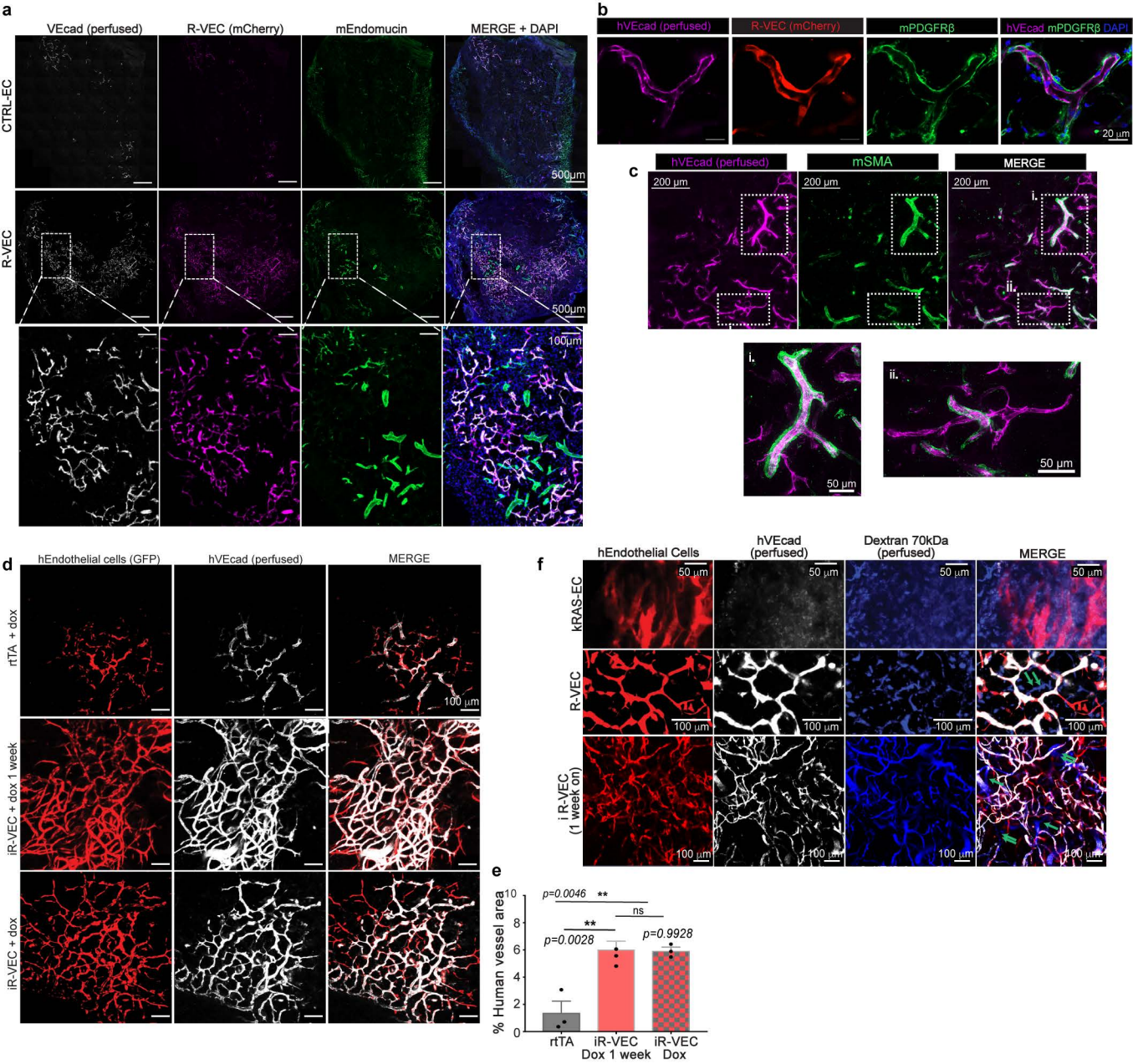
a
VEcad (perfused)
R-VEC (mCherry)
mEndomucin
MERGE + DAPI
CTRL-EC
R-VEC
500µm
500µm
100µm
b
hVEcad (perfused)
R-VEC (mCherry)
mPDGFRβ
hVEcad mPDGFRβ DAPI
20 µm
c
hVEcad (perfused)
mSMA
MERGE
200 µm
200 µm
200 µm
i.
ii.
i.
50 µm
ii.
50 µm
d
hEndothelial cells (GFP)
hVEcad (perfused)
MERGE
rtTA + dox
iR-VEC + dox 1 week
iR-VEC + dox
100 µm
e
% Human vessel area
p=0.0046
**
ns
**
p=0.0028
p=0.9928
rtTA
iR-VEC Dox 1 week
iR-VEC Dox
f
hEndothelial Cells
hVEcad (perfused)
Dextran 70kDa (perfused)
MERGE
kRAS-EC
R-VEC
iR-VEC (1 week on)
50 µm
100 µm

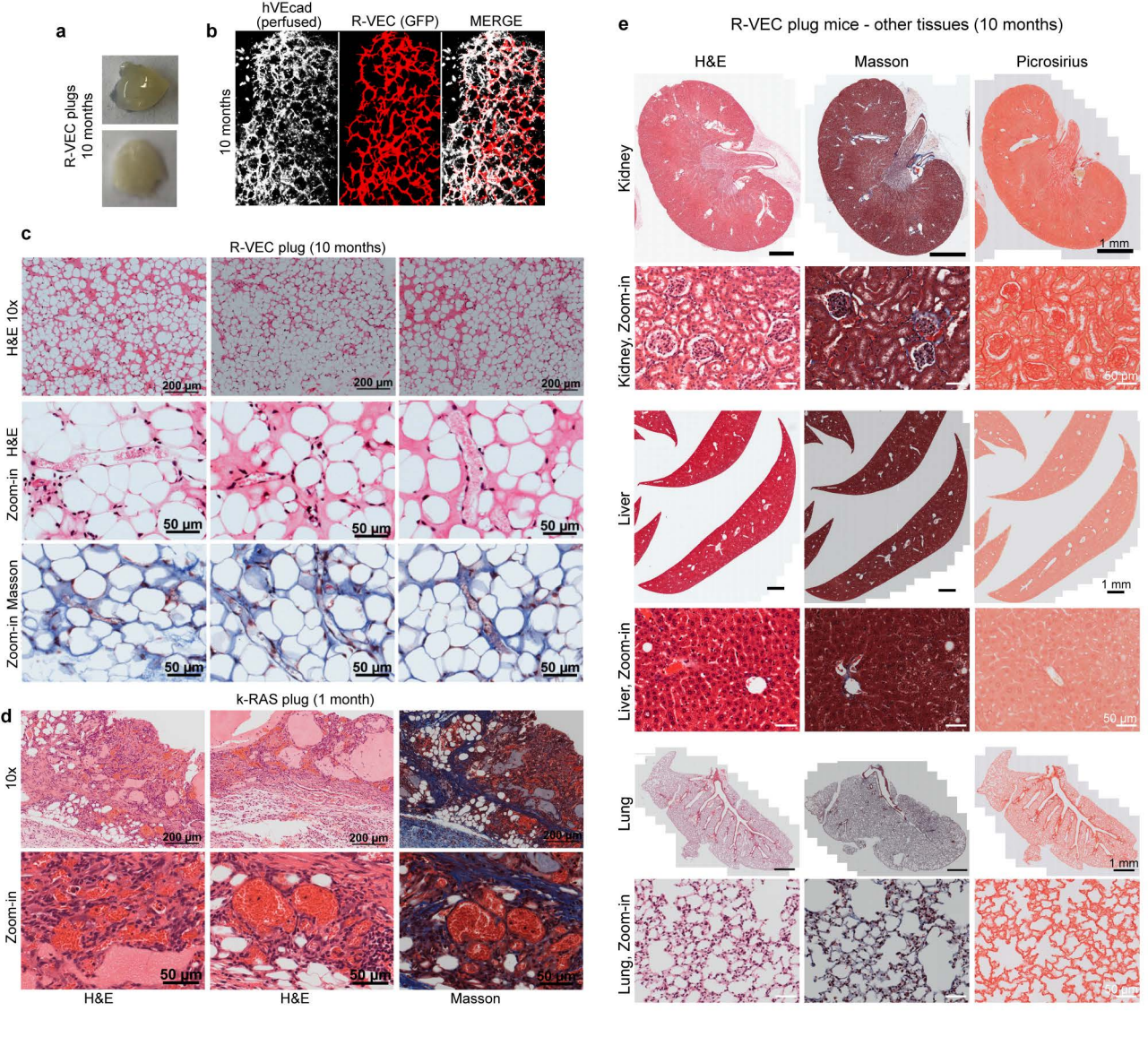
a
R-VEC plugs
10 months
b
hVEcad
(perfused)
R-VEC (GFP)
MERGE
10 months
c
R-VEC plug (10 months)
H&E 10x
Zoom-in H&E
Zoom-in Masson
200 µm
50 µm
d
k-RAS plug (1 month)
10x
Zoom-in
H&E
H&E
Masson
e
R-VEC plug mice - other tissues (10 months)
H&E
Masson
Picrosirius
Kidney
Kidney, Zoom-in
Liver
Liver, Zoom-in
Lung
Lung, Zoom-in
1 mm
50 µm

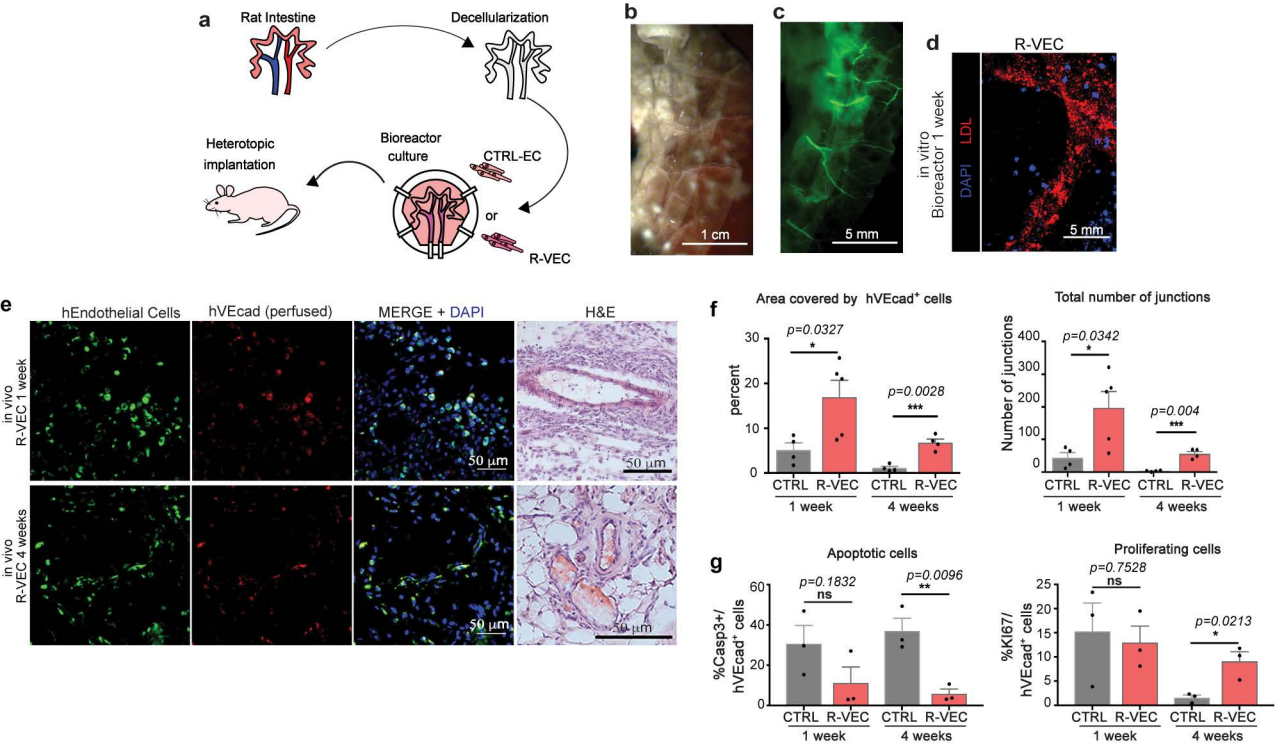
a
Rat Intestine
Decellularization
Heterotopic implantation
Bioreactor culture
CTRL-EC
or
R-VEC
b
1 cm
c
5 mm
d
R-VEC
in vitro Bioreactor 1 week
LDL
DAPI
5 mm
e
hEndothelial Cells
hVEcad (perfused)
MERGE + DAPI
H&E
in vivo R-VEC 1 week
in vivo R-VEC 4 weeks
50 µm
f
Area covered by hVEcad+ cells
percent
p=0.0327
p=0.0028
CTRL
R-VEC
1 week
4 weeks
Total number of junctions
Number of junctions
p=0.0342
p=0.004
g
Apoptotic cells
%Casp3+/ hVEcad+ cells
p=0.1832
ns
p=0.0096
Proliferating cells
%KI67/ hVEcad+ cells
p=0.7528
p=0.0213

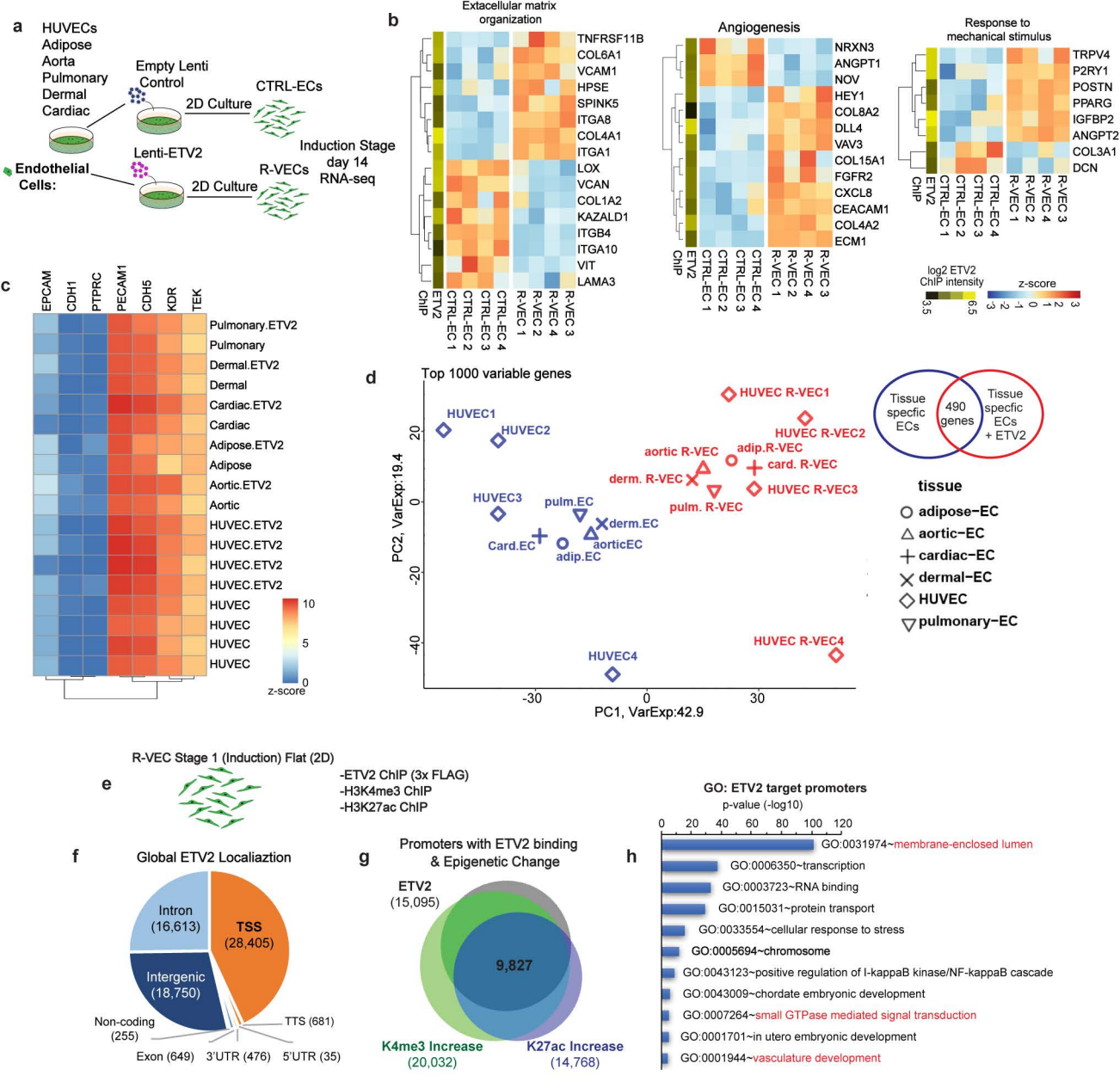
a
HUVECs
Adipose
Aorta
Pulmonary
Dermal
Cardiac
Empty Lenti Control
2D Culture
CTRL-ECs
Lenti-ETV2
Endothelial Cells:
2D Culture
R-VECs
Induction Stage day 14 RNA-seq
b
Extracellular matrix organization
TNFRSF11B
COL6A1
VCAM1
HPSE
SPINK5
ITGA8
COL4A1
ITGA1
LOX
VCAN
COL1A2
KAZALD1
ITGB4
ITGA10
VIT
LAMA3
Angiogenesis
NRXN3
ANGPT1
NOV
HEY1
COL8A2
DLL4
VAV3
COL15A1
FGFR2
CXCL8
CEACAM1
COL4A2
ECM1
Response to mechanical stimulus
TRPV4
P2RY1
POSTN
PPARG
IGFBP2
ANGPT2
COL3A1
DCN
ChIP
ETV2
CTRL-EC 1
CTRL-EC 2
CTRL-EC 3
CTRL-EC 4
R-VEC 1
R-VEC 2
R-VEC 4
R-VEC 3
log2 ETV2 ChIP intensity
3.5
6.5
z-score
-3
-2
-1
0
1
2
3
c
EPCAM
CDH1
PTPRC
PECAM1
CDH5
KDR
TEK
Pulmonary.ETV2
Pulmonary
Dermal.ETV2
Dermal
Cardiac.ETV2
Cardiac
Adipose.ETV2
Adipose
Aortic.ETV2
Aortic
HUVEC.ETV2
HUVEC.ETV2
HUVEC.ETV2
HUVEC.ETV2
HUVEC
HUVEC
HUVEC
HUVEC
10
5
0
z-score
d
Top 1000 variable genes
HUVEC1
HUVEC2
HUVEC3
HUVEC4
HUVEC R-VEC1
HUVEC R-VEC2
HUVEC R-VEC3
HUVEC R-VEC4
aortic R-VEC
adip.R-VEC
card. R-VEC
derm. R-VEC
pulm. R-VEC
pulm.EC
derm.EC
aorticEC
adip.EC
Card.EC
PC2, VarExp:19.4
PC1, VarExp:42.9
20
0
-20
-40
-30
0
30
Tissue specific ECs
490 genes
Tissue specific ECs + ETV2
tissue
adipose−EC
aortic−EC
cardiac−EC
dermal−EC
HUVEC
pulmonary−EC
e
R-VEC Stage 1 (Induction) Flat (2D)
-ETV2 ChIP (3x FLAG)
-H3K4me3 ChIP
-H3K27ac ChIP
f
Global ETV2 Localiaztion
Intron (16,613)
TSS (28,405)
Intergenic (18,750)
Non-coding (255)
TTS (681)
Exon (649)
3'UTR (476)
5'UTR (35)
g
Promoters with ETV2 binding & Epigenetic Change
ETV2 (15,095)
9,827
K4me3 Increase (20,032)
K27ac Increase (14,768)
h
GO: ETV2 target promoters
p-value (-log10)
0
20
40
60
80
100
120
GO:0031974~membrane-enclosed lumen
GO:0006350~transcription
GO:0003723~RNA binding
GO:0015031~protein transport
GO:0033554~cellular response to stress
GO:0005694~chromosome
GO:0043123~positive regulation of I-kappaB kinase/NF-kappaB cascade
GO:0043009~chordate embryonic development
GO:0007264~small GTPase mediated signal transduction
GO:0001701~in utero embryonic development
GO:0001944~vasculature development

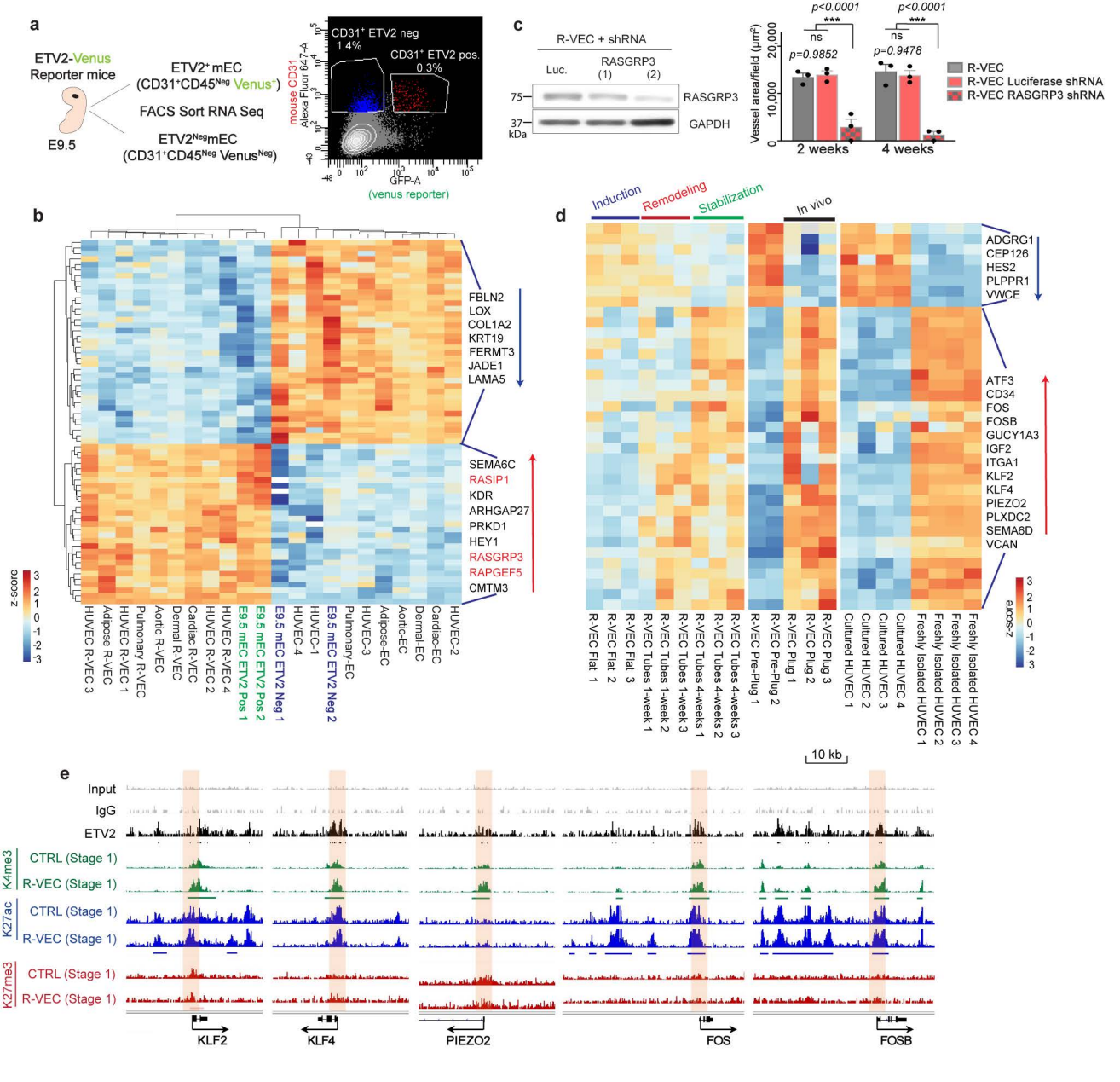
a
ETV2-Venus
Reporter mice
E9.5
ETV2+ mEC
(CD31+CD45Neg Venus+)
FACS Sort RNA Seq
ETV2Neg mEC
(CD31+CD45Neg VenusNeg)
CD31+ ETV2 neg
1.4%
CD31+ ETV2 pos.
0.3%
mouse CD31
Alexa Fluor 647-A
GFP-A
(venus reporter)
c
R-VEC + shRNA
Luc.
RASGRP3
(1)
(2)
75
37
kDa
RASGRP3
GAPDH
p<0.0001
p<0.0001
***
***
ns
ns
p=0.9852
p=0.9478
Vessel area/field (μm²)
20,000
10,000
0
2 weeks
4 weeks
R-VEC
R-VEC Luciferase shRNA
R-VEC RASGRP3 shRNA
b
z-score
3
2
1
0
-1
-2
-3
FBLN2
LOX
COL1A2
KRT19
FERMT3
JADE1
LAMA5
SEMA6C
RASIP1
KDR
ARHGAP27
PRKD1
HEY1
RASGRP3
RAPGEF5
CMTM3
HUVEC R-VEC 3
Adipose R-VEC
HUVEC R-VEC 1
Pulmonary R-VEC
Aortic R-VEC
Dermal R-VEC
Cardiac R-VEC
HUVEC R-VEC 2
HUVEC R-VEC 4
E9.5 mEC ETV2 Pos 1
E9.5 mEC ETV2 Pos 2
E9.5 mEC ETV2 Neg 1
E9.5 mEC ETV2 Neg 2
HUVEC-4
HUVEC-1
HUVEC-3
Pulmonary-EC
Adipose-EC
Aortic-EC
Dermal-EC
Cardiac-EC
HUVEC-2
d
Induction
Remodeling
Stabilization
In vivo
ADGRG1
CEP126
HES2
PLPPR1
VWCE
ATF3
CD34
FOS
FOSB
GUCY1A3
IGF2
ITGA1
KLF2
KLF4
PIEZO2
PLXDC2
SEMA6D
VCAN
z-score
3
2
1
0
-1
-2
-3
R-VEC Flat 1
R-VEC Flat 2
R-VEC Flat 3
R-VEC Tubes 1-week 1
R-VEC Tubes 1-week 2
R-VEC Tubes 1-week 3
R-VEC Tubes 4-weeks 1
R-VEC Tubes 4-weeks 2
R-VEC Tubes 4-weeks 3
R-VEC Pre-Plug 1
R-VEC Pre-Plug 2
R-VEC Plug 1
R-VEC Plug 2
R-VEC Plug 3
Cultured HUVEC 1
Cultured HUVEC 2
Cultured HUVEC 3
Cultured HUVEC 4
Freshly Isolated HUVEC 1
Freshly Isolated HUVEC 2
Freshly Isolated HUVEC 3
Freshly Isolated HUVEC 4
e
10 kb
Input
IgG
ETV2
K4me3
CTRL (Stage 1)
R-VEC (Stage 1)
K27ac
CTRL (Stage 1)
R-VEC (Stage 1)
K27me3
CTRL (Stage 1)
R-VEC (Stage 1)
KLF2
KLF4
PIEZO2
FOS
FOSB

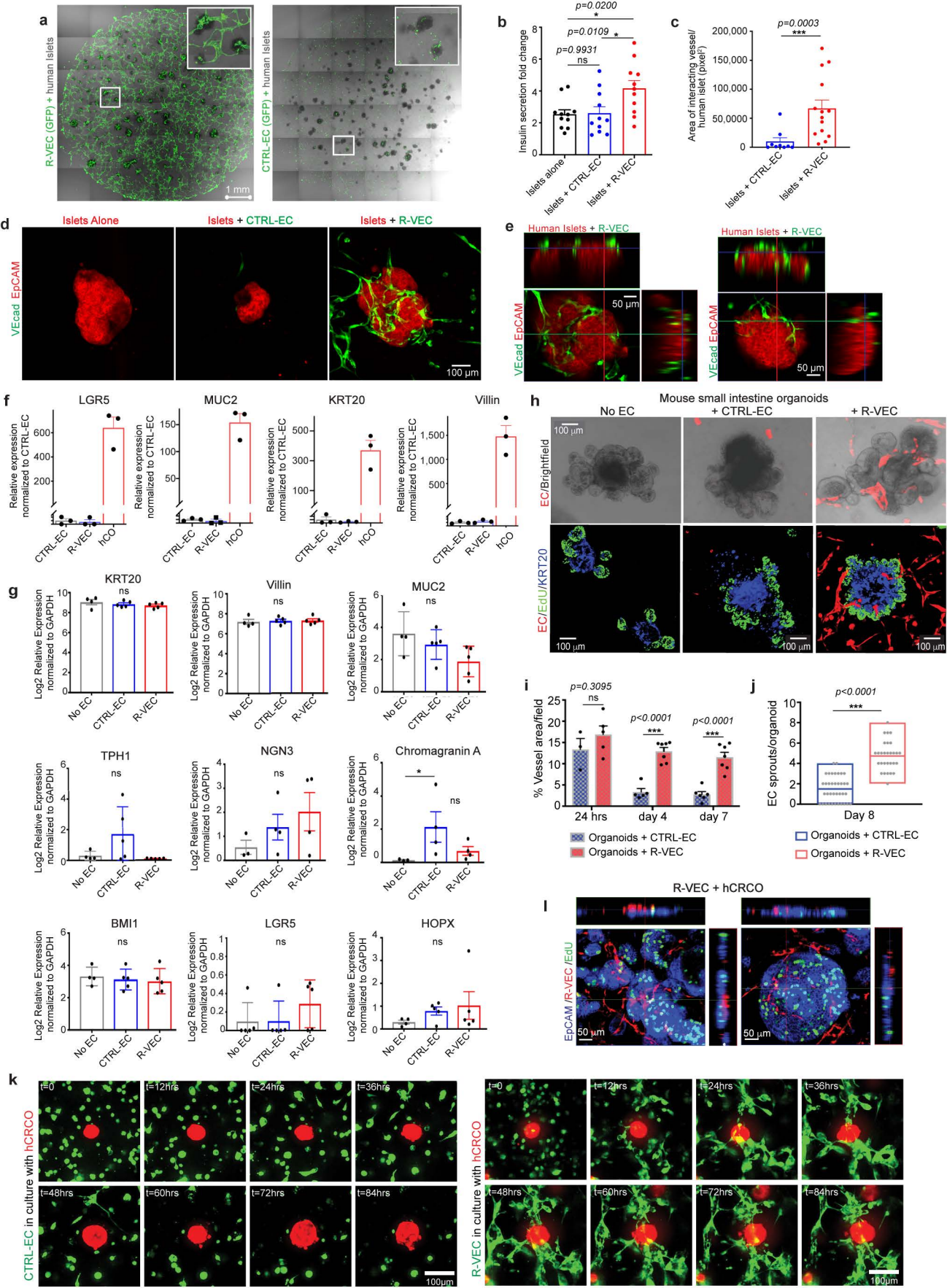
a
R-VEC (GFP) + human Islets
CTRL-EC (GFP) + human Islets
1 mm
b
Insulin secretion fold change
p=0.0200
p=0.0109
p=0.9931
ns
Islets alone
Islets + CTRL-EC
Islets + R-VEC
c
Area of interacting vessel/ human islet (pixel²)
p=0.0003
***
Islets + CTRL-EC
Islets + R-VEC
d
Islets Alone
Islets + CTRL-EC
Islets + R-VEC
VEcad EpCAM
100 µm
e
Human Islets + R-VEC
VEcad EpCAM
50 µm
f
LGR5
MUC2
KRT20
Villin
Relative expression normalized to CTRL-EC
CTRL-EC
R-VEC
hCO
g
KRT20
Villin
MUC2
TPH1
NGN3
Chromagranin A
BMI1
LGR5
HOPX
Log2 Relative Expression normalized to GAPDH
ns
No EC
CTRL-EC
R-VEC
h
Mouse small intestine organoids
No EC
+ CTRL-EC
+ R-VEC
EC/Brightfield
EC/EdU/KRT20
100 µm
i
% Vessel area/field
p=0.3095
p<0.0001
p<0.0001
24 hrs
day 4
day 7
Organoids + CTRL-EC
Organoids + R-VEC
j
EC sprouts/organoid
p<0.0001
Day 8
Organoids + CTRL-EC
Organoids + R-VEC
k
CTRL-EC in culture with hCRCO
R-VEC in culture with hCRCO
t=0
t=12hrs
t=24hrs
t=36hrs
t=48hrs
t=60hrs
t=72hrs
t=84hrs
100µm
l
R-VEC + hCRCO
EpCAM /R-VEC /EdU
50 µm

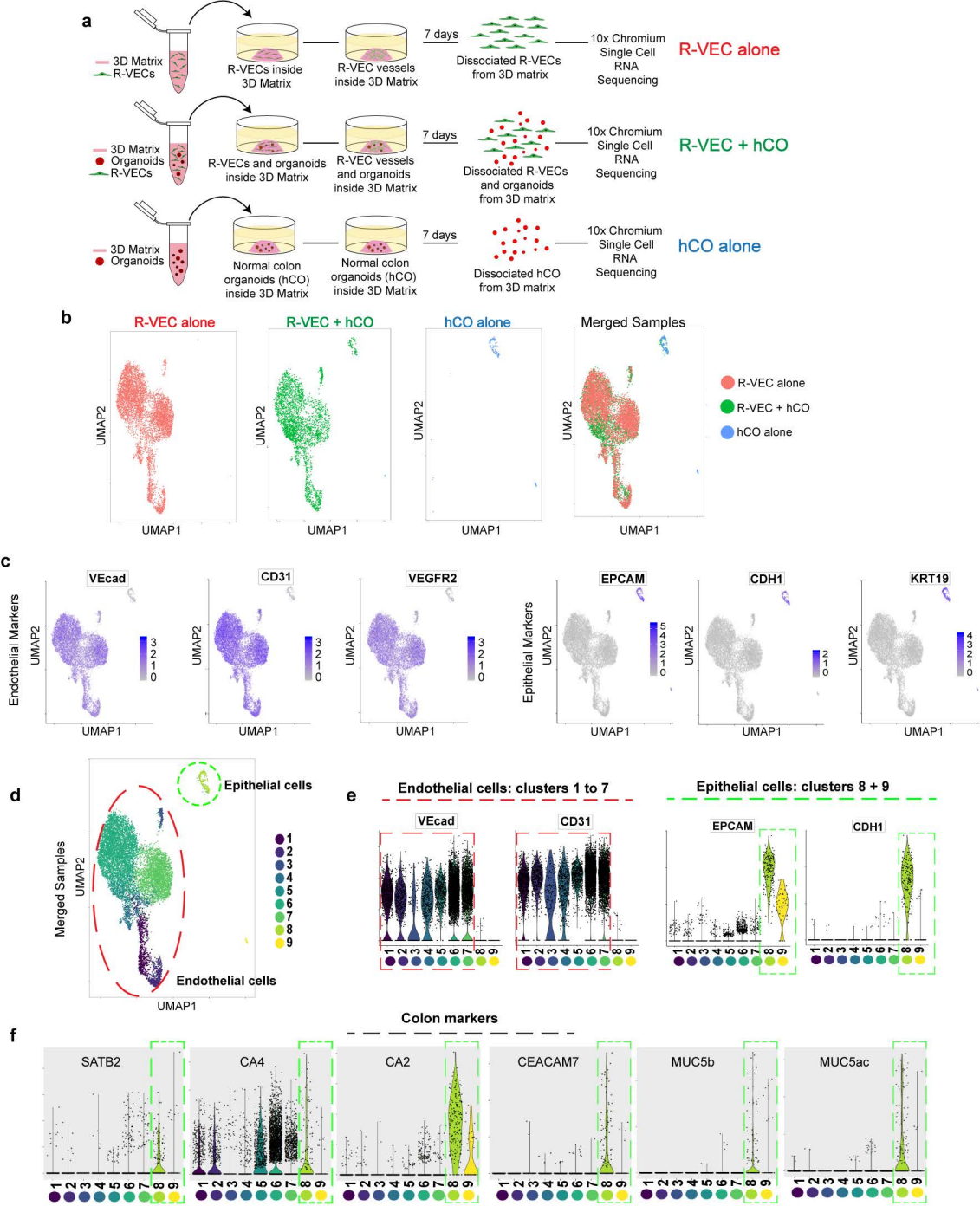
a
3D Matrix
R-VECs
R-VECs inside 3D Matrix
R-VEC vessels inside 3D Matrix
7 days
Dissociated R-VECs from 3D matrix
10x Chromium Single Cell RNA Sequencing
R-VEC alone
3D Matrix
Organoids
R-VECs
R-VECs and organoids inside 3D Matrix
R-VEC vessels and organoids inside 3D Matrix
7 days
Dissociated R-VECs and organoids from 3D matrix
10x Chromium Single Cell RNA Sequencing
R-VEC + hCO
3D Matrix
Organoids
Normal colon organoids (hCO) inside 3D Matrix
Normal colon organoids (hCO) inside 3D Matrix
7 days
Dissociated hCO from 3D matrix
10x Chromium Single Cell RNA Sequencing
hCO alone
b
R-VEC alone
R-VEC + hCO
hCO alone
Merged Samples
UMAP1
UMAP2
R-VEC alone
R-VEC + hCO
hCO alone
c
Endothelial Markers
Epithelial Markers
VEcad
CD31
VEGFR2
EPCAM
CDH1
KRT19
UMAP1
UMAP2
d
Epithelial cells
Endothelial cells
Merged Samples
UMAP1
UMAP2
e
Endothelial cells: clusters 1 to 7
Epithelial cells: clusters 8 + 9
VEcad
CD31
EPCAM
CDH1
f
Colon markers
SATB2
CA4
CA2
CEACAM7
MUC5b
MUC5ac

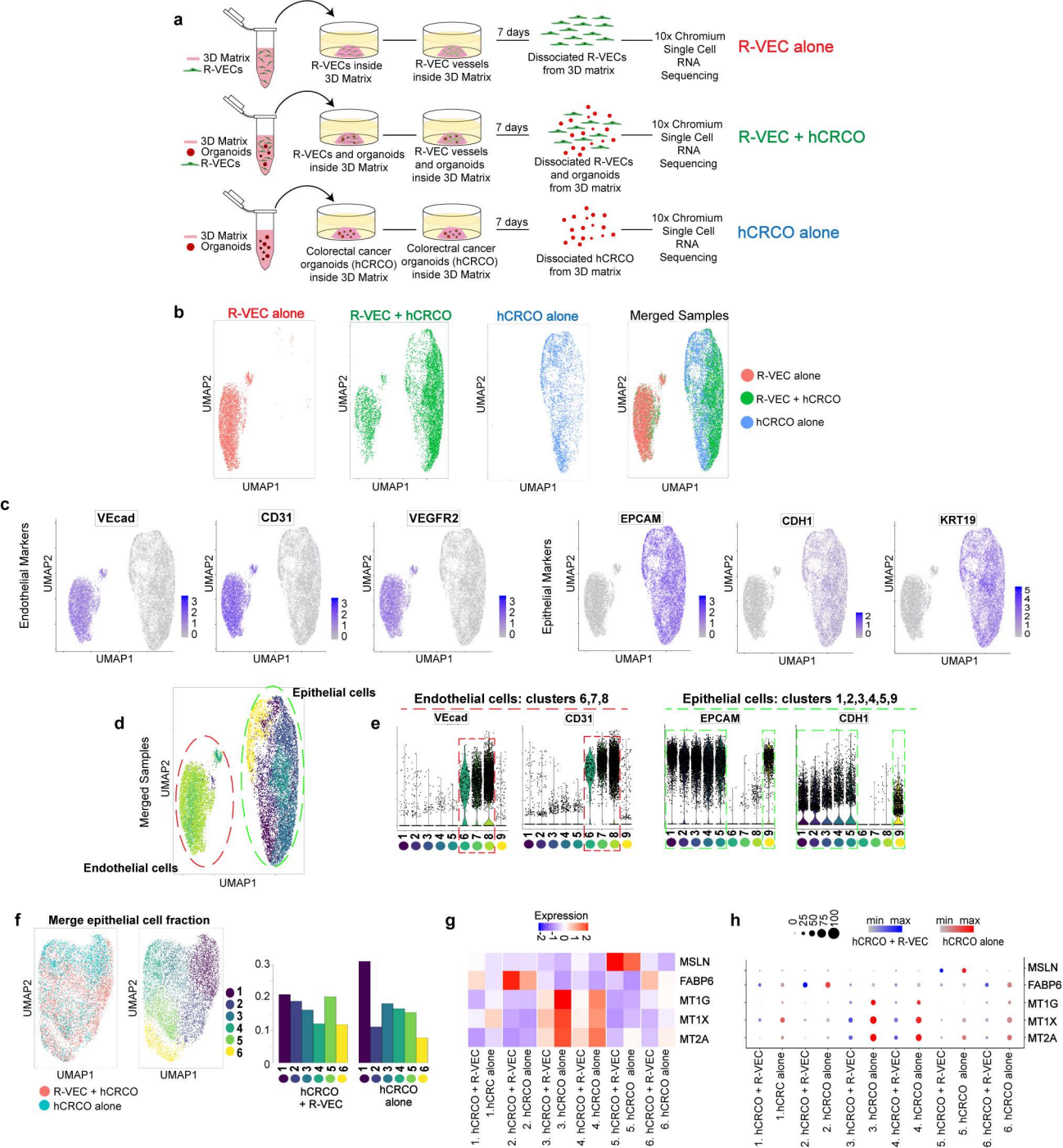
a
3D Matrix
R-VECs
R-VECs inside 3D Matrix
R-VEC vessels inside 3D Matrix
7 days
Dissociated R-VECs from 3D matrix
10x Chromium Single Cell RNA Sequencing
R-VEC alone
3D Matrix
Organoids
R-VECs
R-VECs and organoids inside 3D Matrix
R-VEC vessels and organoids inside 3D Matrix
7 days
Dissociated R-VECs and organoids from 3D matrix
10x Chromium Single Cell RNA Sequencing
R-VEC + hCRCO
3D Matrix
Organoids
Colorectal cancer organoids (hCRCO) inside 3D Matrix
Colorectal cancer organoids (hCRCO) inside 3D Matrix
7 days
Dissociated hCRCO from 3D matrix
10x Chromium Single Cell RNA Sequencing
hCRCO alone
b
R-VEC alone
R-VEC + hCRCO
hCRCO alone
Merged Samples
UMAP1
UMAP2
R-VEC alone
R-VEC + hCRCO
hCRCO alone
c
Endothelial Markers
Epithelial Markers
VEcad
CD31
VEGFR2
EPCAM
CDH1
KRT19
UMAP1
UMAP2
d
Merged Samples
Epithelial cells
Endothelial cells
e
Endothelial cells: clusters 6,7,8
Epithelial cells: clusters 1,2,3,4,5,9
VEcad
CD31
EPCAM
CDH1
f
Merge epithelial cell fraction
R-VEC + hCRCO
hCRCO alone
hCRCO + R-VEC
hCRCO alone
g
Expression
MSLN
FABP6
MT1G
MT1X
MT2A
1. hCRCO + R-VEC
1.hCRC alone
2. hCRCO + R-VEC
2. hCRCO alone
3. hCRCO + R-VEC
3. hCRCO alone
4. hCRCO + R-VEC
4. hCRCO alone
5. hCRCO + R-VEC
5. hCRCO alone
6. hCRCO + R-VEC
6. hCRCO alone
h
min max
hCRCO + R-VEC
min max
hCRCO alone
MSLN
FABP6
MT1G
MT1X
MT2A